https://doi.org/10.5194/wes-2026-23
Preprint. Discussion started: 20 February 2026

eawe european academy of wind energy
Open Access WIND ENERGY SCIENCE DISCUSSIONS

Mitigation of offshore wind farm cluster wake effects by low-specific-rating, low-induction turbines

Johannes Paulsen[1,2], Gerald Steinfeld[1,2], Martin Kühn[1,2], and Martin Dörenkämper[3]

[1]Carl von Ossietzky Universität Oldenburg, School of Mathematics and Science, Institute of Physics
[2]ForWind - Center for Wind Energy Research, Küpkersweg 70, 26129 Oldenburg, Germany
[3]Fraunhofer IWES, Küpkersweg 70, 26129 Oldenburg, Germany

Correspondence: Johannes Paulsen (johannes.paulsen@uni-oldenburg.de)

Abstract. One of the major challenges for the large-scale expansion of offshore wind energy across several countries is the strong interaction between wind farm clusters within designated areas of high power density. The resulting cluster wake effects significantly reduce the annual energy production, especially during periods with low to medium wind speeds.

We analyse a potential mitigation strategy by comparing prospective expansion scenarios for the entire available area in the German Bight, employing a low-specific-rating, low-induction turbine concept, against a conventional 15 MW reference design. While maintaining the rated power and wind farm layout, the innovative turbine, denoted the hybrid-lambda concept, has a 35 % larger rotor diameter with a corresponding higher hub height than the reference machine and a significantly reduced thrust coefficient above 6.8 ms^{-1}.

We perform mesoscale simulations with the induction-modified Fitch wind farm parametrisation for one entire year, representative of multi-decadal wind speed and direction statistics. We investigate boundary-layer interaction, inner- and inter-wind-farm wake effects, as well as power performance over the entire year and during critical grid situations, such as doldrums.

Maintaining a prescribed power density, the low-specific-rating, low-induction turbine provides an increase of 19.4 % in annual energy generation, the corresponding capacity factor, and the number of full-load hours compared to the conventional concept. The surplus is mainly caused by the larger swept rotor area, rather than by the increased hub height and the reduced inner-farm wake effects due to the low-induction rotor design, while we observed stronger wind speed deficits outside of the clusters.

Especially during periods of very low power production, our results show lower cluster-wake-induced wind speed reductions and higher generated power with lower fluctuations from hybrid-lambda turbines. In consequence, doldrums, i.e. periods when the total generated power of the German Bight is below a certain fraction of the installed power, are less frequent and have shorter duration.

In another simulation variant, the number and total installed power of the hybrid-lambda turbines were reduced by 22.0 % while still achieving the same energy output as generated by the original number of conventional turbines. Additional simulation setups show a lower decrease in performance in the German sector equipped with hybrid-lambda turbines compared to the reference when adding additional wind farm clusters in the prevailing wind direction within the Dutch exclusive economic zone. We conclude that the deployment of such innovative low-specific-rating, low-induction turbines can provide higher en-

https://doi.org/10.5194/wes-2026-23
Preprint. Discussion started: 20 February 2026

eawe european academy of wind energy
Open Access WIND ENERGY SCIENCE DISCUSSIONS

ergy production at a prescribed power density or require a smaller number of installed turbines to achieve a given annual energy production especially in dense area with significant cluster wake effects. Overall, such turbines feature higher feed-in at low wind speeds and more stable power output, requiring less reserve power and possibly contributing to improved grid stability.

1 Introduction

Many challenges accompany the large-scale deployment of offshore wind energy. One of them, especially crucial for some countries, e.g. Germany or Belgium, is the comparatively large spatial density of installed power planned for the near future. The German government plans to reach 70 GW of installed power by 2045 in the German exclusive economic zone (EEZ) in the North Sea, which requires an increase of more than 59 GW compared to the capacity installed by autumn 2025.

Another challenge arising with the growing penetration of wind power in the electricity mix is the so-called "self-cannibalization" of wind energy, i.e. decreasing prices during strong wind speeds, thus reducing the economic value of the wind energy turbines (López Prol et al., 2020; May et al., 2015). Further, substantial penetration of intermittent energy supply, such as wind power, generates an increased demand for the provision of ancillary services (i.e. Frequency Containment Reserve, Automatic Frequency Restoration Reserve and Minute Reserve). This means a financial burden for the grid operators and the government, amounting to a total cost of 500 Mio. Euros in 2024 (Bundesnetzagentur, 2025). For onshore wind energy, Hirth and Müller (2016) show that advanced turbine concepts with larger rotors and hence lower specific ratings can provide benefits in that regard, using a techno-economic model for energy generation and dispatch. They observe an increase in the value of wind energy by up to 15 % at 30 % penetration of wind energy in an energy system.

Next to these grid-related challenges, the greater wind farm density and higher power density within the wind farms in the German EEZ leads to a high degree of interaction between the wind farm clusters. While the annual energy production (AEP) within the entire German Bight is enhanced with the number of turbines, the capacity factor (CF) and full load hours (FLH) are decreased with more wind farms, due to - among other things - the more frequent occurrence and heightened strength of cluster wakes (Dörenkämper et al., 2023).

Fliegner et al. (2025) analysed one proposal of mitigating cluster wakes, by distributing the installed turbines in the North Sea more equally across national borders. Assessing the turbulent kinetic energy budget in the lower atmosphere, they show that by adhering to national borders and current policies, wake induced losses of up to 30 % are expected. Positioning the wind turbines more balanced across the Dutch, German and Danish EEZ could reduce wake losses by up to 18 %. While the modelling approach applied by Fliegner et al. (2025) assumes homogeneous distribution of wind farms across large boxes, their insights show promise for cross-border collaboration especially between the Netherlands, Germany and Denmark.

Another idea to reduce the strength of wind farm (cluster) wakes is the application of wind farm control concepts. While they classically aimed at increasing the efficiency of single wind farms, reducing loads and providing grid services (Meyers

https://doi.org/10.5194/wes-2026-23
Preprint. Discussion started: 20 February 2026

eawe european academy of wind energy
Open Access WIND ENERGY SCIENCE DISCUSSIONS

et al., 2022), a collaboration on optimising the interaction between different wind farm clusters rather than just optimising on wind farm level could provide benefits (Foloppe et al., 2023). One new concept introduced by Gutknecht et al. (2024) aims at mitigating wake effects at the level of entire wind farm clusters. Their approach at actively mixing cluster wakes (Active Cluster Wake Control, ACWC) proposes a temporally and spatially varying wind turbine thrust throughout the entire wind farm cluster. While large eddy simulations (LES) show a decreased cluster wake strength with ACWC applied, power gains for the cluster itself are only observed during laminar inflow.

Regarding the turbines employed within one wind farm, also several aspects have been analysed in previous studies. Here, Syed et al. (2020) analysed the possible placement of turbines with different hub heights inside one wind farm, a concept also called vertical staggering. Using mesoscale simulations, they found that the approach of vertical staggering reduces the overlap of wind turbine wakes and hence leads to a higher power production. In another study, Kasper and Stevens (2024) investigate the effect of rotor tilt on inner farm wind wakes. They observed, that a rotor tilt of -20 ° reduces inter- and inner-farm wakes and can improve the combined wind farm efficiency of two aligned wind farms by up to 11 %.

A fourth approach of mitigating the impact of increasing strength of wind farm wakes is the installation of low-specific rating turbines, i.e. turbines with a smaller ratio of rated power to the rotor diameter or of different aerodynamic turbine designs, especially with lower rotor induction. Novel rotor design concepts with disruptively low specific ratings have been proposed mainly for onshore use (e.g. Madsen et al., 2020; Bortolotti et al., 2021). At the example of a 10 MW offshore turbine, Chaviaropoulos and Sieros (2014) suggest, that reducing the blades' axial induction factor from a=0.33 to a=0.2 and increasing the rotor diameter by 13 % could result in an AEP increase of 3.5 % and a thrust reduction of 10 % on a single turbine level.

Aiming at minimizing the levelised cost of energy (LCoE), Mehta et al. (2024) employed a multi-disciplinary design optimization and analysis (MDAO) framework to optimise the size and the specific rating of offshore turbines while maintaining the rotor induction and associated thrust coefficient. The baseline optimisation for an area constrained wind farm with 1 GW of installed power yields a specific turbine rating of 366 Wm^{-2}, which is close to the value of the IEA 15 MW reference turbine and the current market trend. The sensitivity to various turbine, operational and maintenance, farm level and site parameters is systematically studied. At locations with lower wind speeds, the LCoE optimisation shows a tendency to decreasing the specific rating. Further, when optimizing on the AEP instead of the LCoE or constraining the farm power instead of the farm area, lower specific ratings are found to be beneficial as well. In contrast, other design conditions, e.g. increasing the power density of the farm or constraining the farm area rather than farm power, favour higher-specific-rating turbines. Quinn et al. (2016) applied engineering models together with a generalised cost model for an offshore wind farm with 1 GW of installed power and found a decreased LCoE for the low-induction, lower specific rating wind turbine AVATAR, compared to a conventional turbine with the same rated power of 10 MW. Here, the results also provide an indication that with the same layout configuration, an increase of 8 % in the capacity factor can be achieved for the AVATAR turbine. Further, to achieve the same AEP, a wind farm with low induction rotors needs less space than the same wind farm with conventional turbine concepts.

Recently, Ribnitzky et al. (2024) introduced the hybrid-lambda (HL) turbine. The HL concept is a low-specific-rating, low-induction turbine, designed particularly for offshore deployment. The enlarged rotor diameter of the turbine, together with a new control approach, i.e. implementing two distinct operating modes (low wind and strong wind) in the partial load range,

https://doi.org/10.5194/wes-2026-23
Preprint. Discussion started: 20 February 2026

eawe european academy of wind energy
Open Access WIND ENERGY SCIENCE DISCUSSIONS

promise an increased energy yield, especially at low wind speeds. Previous studies on this innovative rotor concept indicate positive impacts concerning power production and wake development for single turbines, two turbines (Ribnitzky et al., 2023) and also in a wind farm setup (Paulsen et al., 2024). For single turbines, Ribnitzky et al. (2024) found an increase in AEP of 11 % at a typical future site in the German Bight (annual average wind speed v_{ave} = 10.2 ms^{-1}) and 21 % at the cluster-wake affected FINO1 location (v_{ave} = 7.9 ms^{-1}) compared to the conventional IEA-15 MW turbine introduced by Gaertner et al. (2020). Using Large-Eddy and Free Vortex Wake simulations, Ribnitzky et al. (2023) showed beneficial turbine wake development, especially when operating in strong wind mode below the rated wind speed. Further, the study also reveals an increase of energy generation of a two-turbine-setup with same absolute spacing compared to two IEA-15 MW turbines, especially at stable stratification.

On larger scales and across an entire year, i.e. on wind farm cluster level, Paulsen et al. (2024) observe an increase of 15 % in the AEP, demonstrating additional benefits of the HL turbines in such a setting compared to the above-mentioned performance with free inflow at turbine level reported by Ribnitzky et al. (2024). Considering the development cluster wakes, Paulsen et al. (2024) observe more pronounced wakes during low wind speeds for the HL-cluster. When transitioning to strong wind mode, the thrust coefficient of the HL turbine drops significantly and the wakes of both, HL- and IEA-cluster are very similar. At high wind speeds, above rated, the cluster wake deficit for the HL-cluster is much lower compared to the IEA-cluster. During specific situations with stable stratification the power production of the HL-cluster shows an increase of 86 % when operating at low wind speed, which further increases to 100 % when switching to strong wind mode.

As previously discussed, the scarcely available space in the German North Sea is set to be equipped very densely with offshore wind farms. In Dörenkämper et al. (2023), the authors supported the development of a site development plan for German offshore areas, where based on Germany's installation goals and available areas possible wind farm clusters are equipped with turbines. The presented scenarios incorporate different offshore wind turbine sizes, based on the current and predicted market trend, including large future turbines with rated powers of 15 MW and 22 MW respectively. The authors use mesoscale simulations to estimate the energy yield and efficiency of the wind farm clusters. The applied simulation setup is also used in this paper.

To perform such mesoscale simulations and analyse the interaction of large wind farm clusters with the atmospheric boundary layer (ABL) and each other different wind farm parametrisations were introduced (e.g. Fitch et al., 2012; Volker et al., 2015; Redfern et al., 2019; Pan and Archer, 2018). Studies compare different WFPs within the mesoscale Weather Research and Forecasting (WRF) model (e.g. Ali et al., 2023; Fischereit et al., 2022) revealing good agreement for wind speed deficits within all parametrisations and slight advantages for the Fitch et al. (2012) parametrisation with regard to the generation of turbulence kinetic energy (TKE). Recently, Cañadillas et al. (2022) pointed out that the wind speed statistics across long time series are predicted very well from the Fitch WFP within the WRF model, with the average difference to lidar measurements being only 2 %. However, Vollmer et al. (2024) showed, that especially for turbines who are placed in a grid cell on their own, the power production of the turbines is overestimated due to the neglected axial induction of the turbines themselves. While this effect is observed to almost cancel out with wake effects for multiple turbines per grid cell, a great impact manifests when very few or even just one turbine is placed per grid cell in the model domain. To mitigate the effect, the authors introduced a novel

https://doi.org/10.5194/wes-2026-23
Preprint. Discussion started: 20 February 2026

eawe european academy of wind energy
Open Access WIND ENERGY SCIENCE DISCUSSIONS

axial induction correction to the model. Further, Sengers et al. (2024) demonstrated, that the standard Fitch WFP without the above mentioned modification overestimates the wake losses for wind farms in situations with a comparatively low turbulence intensity (TI) by up to 30.8 %. The new induction correction however, leads to very well represented internal and external wakes, while still slightly underestimating the turbines power production when compared to operational data (Sengers, 2025).

Particularly for regions with dense installation plans of offshore wind power — like the German Bight — there is limited understanding of how large-scale deployment of different turbine concepts influences inter-cluster wakes and the overall feed-in characteristics of offshore wind power. Additionally, the behaviour of different turbine types under challenging conditions, such as doldrums, i.e. periods of low wind, is still to be analysed. Addressing these gaps is crucial for showing ways in which the reliability and efficiency of offshore wind energy systems can be improved.

The objective of this study is to compare a new and innovative low-specific-rating turbine design with a conventional turbine concept regarding the development of cluster wakes, wind farm (cluster) efficiency, and the temporal characteristics of power production. Here, we aim at assessing the feed-in characteristics of these turbines across an entire year as well as during challenging grid situations, e.g. doldrums or with reduced power density across all wind farm clusters. Further, the study addresses the impacts of large scale expansion of offshore wind energy in neighbouring countries on the performance of wind farm cluster in the German EEZ.

Section 2 provides an insight into the simulation set-up (Sec. 2.1), the different turbine concepts (Sec. 2.2), the different approaches of turbine placements within the German North Sea (Sec. 2.3) used for this study. In Section 3 we present our results, before discussing them in Section 4. Section 5 provides a summary of our findings and provides an outlook on future studies.

2 Methods

The following section gives an overview about the mesoscale model WRF used to perform our simulations and its parametrisation. Further, a detailed comparison of the used turbine concepts, i.e. the IEA-15 MW turbine including all the modifications performed for this study and the HL turbine is provided. Subsequently, the exploited areas as well as the layout generation for the different scenarios considered for our study are presented. Lastly, the methodologies of computing the rotor equivalent wind speed (REWS) from the simulated wind fields, normalizing the wind speed with reference wind speeds and separating the gathered data according to different meteorological situations, coinciding with e.g. different operation modes of the turbines are presented together with the different metrics we apply to compare the performance of the different design concepts.

2.1 Simulation set-up

For our study, we use the mesoscale model WRF version 4.5.1 (Skamarock et al., 2021). We set up our simulation domains to work with three one-way-nested domains with horizontal resolutions of 18 km, 6 km and 2 km respectively. The domains are centred around the German Bight, i.e. our region of interest. Figure 1a depicts the three nested domains with the European coastlines with Fig. 1b showing a close-up of the innermost domain in which the wind farms are parametrised. To drive our

https://doi.org/10.5194/wes-2026-23
Preprint. Discussion started: 20 February 2026

simulations, we use ERA5 (C3S, 2018) and OSTIA (Good et al., 2020) datasets and apply grid nudging in the outermost domain with nudging intervals of 360 min.

Vertically, we discretise our domain into 61 eta levels with the highest altitude level located at 5000 Pa. The vertical levels are defined in such a way that we have 10 and 11 levels across the rotor-swept area of IEA and HL turbines respectively. Further simulation details about the different parametrisations used in our simulations are given in Table 1.

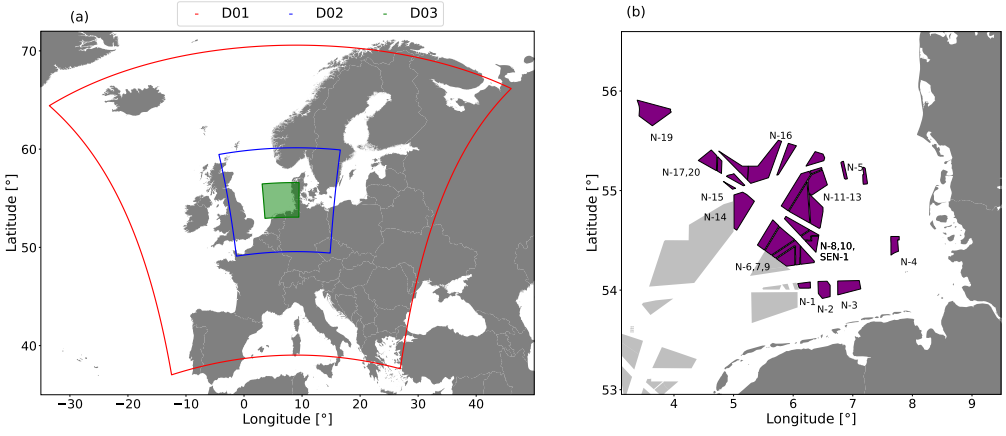

Figure 1. Configuration of the three nested domains in WRF (a) with a close-up of the innermost domain in (b). Here, the parametrised wind farm clusters are depicted in purple (German) and grey (Dutch).

Table 1. Basic settings for the initialization of the simulation.

WRF-Version	4.5.1 (Skamarock et al., 2021)
Initial & boundary conditions	6h ERA5 reanalysis data (C3S, 2018), 6 h OSTIA SST data (Good et al., 2020)
Spin-up time	24 h
Nesting	3 domains, one-way
Horizontal resolution	18 km, 6 km, 2 km
Vertical resolution	61 eta levels
ABL parametrisation	MYNN-2.5 level (Nakanishi and Niino, 2009)
WFP	Induction modified Fitch parametrisation (Vollmer et al., 2024)
Surface layer model	MYNN scheme (Olson et al., 2021)
Radiation	RRTMG (Iacono et al., 2008)

Regarding the simulated time frame, we choose the year 2006 for all scenarios in this study, as Dörenkämper et al. (2023) show that this year represents the long-term wind statistics from 1950 through 2020 in the German Bight very well.

For efficient use of computational resources, we split the year into 37 runs of 10 days each, following a similar procedure like Dörenkämper et al. (2020). Each single run is started with a 24 h spin-up time, ensuring a fully developed flow.

https://doi.org/10.5194/wes-2026-23
Preprint. Discussion started: 20 February 2026

eawe european academy of wind energy
Open Access WIND ENERGY SCIENCE DISCUSSIONS

To represent the wind turbines in our model, we use the induction-modified Fitch parametrisation, developed by Vollmer et al. (2024). In contrast to the original Fitch parametrisation introduced by Fitch et al. (2012), this version also recognises the axial induction of single turbines, providing a more accurate estimation of power production and wake development.

2.2 Turbine concepts

In the scenario simulations, we use two different conceptual turbines, both with a rated power of $P_\mathrm{r} = 15\,\mathrm{MW}$. The IEA-15 MW turbine features a conventional design with a hub height of $z_\mathrm{hub} = 150\,\mathrm{m}$ and a rotor diameter of $D = 240\,\mathrm{m}$ resulting in a specific rating of $P_\mathrm{spec} = P_\mathrm{r} \,/\, \pi(0.5D)^2 = 332\,\mathrm{Wm}^{-2}$. This design thus lies within the span of the current trend in offshore wind turbine development, where specific ratings between $313\,\mathrm{Wm}^{-2}$ and $346\,\mathrm{Wm}^{-2}$ are expected (McCoy et al., 2024). In contrast to the market trend, the new HL concept, developed within the Cooperative Research Centre 1463 Offshore Megastructures, features a larger rotor diameter of $D = 326\,\mathrm{m}$ and an increased hub height of $z_\mathrm{hub} = 193\,\mathrm{m}$. This results in a significantly lower specific rating of $P_\mathrm{spec} = 180\,\mathrm{Wm}^{-2}$.

The blade design of the new concept is load-optimised with a lower induction factor a as the aerodynamic out-of-plane bending moment is kept constant despite the 35 % larger blade length (Ribnitzky et al., 2022). Therefore, the blades feature an almost conventional design in the inner 70 % of their length, while the outer 30 % are very slender.

As Burton (2009) explains, following momentum theory, both the power coefficient c_P and thrust coefficient c_T depend on the axial induction factor a:

$$c_T = 4a \cdot (1 - a) \tag{1}$$

$$c_P = 4a \cdot (1 - a)^2. \tag{2}$$

From these equations it can be seen that the thrust coefficient scales quadratically with the induction factor, while the power coefficient scales with the induction factor cubed. This indicates that a decrease in a has a larger impact on the thrust of a wind turbine than on the power production. Additionally, the lower induction factor and hence also thrust coefficient, lead to less pronounced wake deficits at the end of the near wake, where the relative wake deficit

$$\frac{u_\mathrm{wake}}{u_\infty} = \sqrt{1 - c_T} \tag{3}$$

is driven by the thrust coefficient. Here, u_wake denotes the wind speed in the wake centre and u_∞ the undisturbed inflow wind speed. Moreover, the low induction concept is especially useful for large rotor diameters, as Tyagi and Schmitz (2024) explain that the aerodynamic out-of-plane bending moments, which are a determining factor for dimensioning the blade structure, decrease with the induction factor as well.

Besides the design of the blades, also the control strategy of the HL concept follows a new approach. At low wind speeds from cut-in up to $6.8\,\mathrm{ms}^{-1}$, the turbine operates in the light-wind mode. Here, the tip speed ratio (TSR) is set to 11 and the turbine operates with maximum aerodynamic efficiency, since the outer 30 % of the blades are optimised for light winds at this high TSR. For higher wind speeds the turbine switches to the strong wind mode. To constrain the stationary aerodynamic out-of-plane bending moment to the value of the IEA-15 MW reference design, the blades are pitched towards feather and the

https://doi.org/10.5194/wes-2026-23
Preprint. Discussion started: 20 February 2026

eawe european academy of wind energy
Open Access WIND ENERGY SCIENCE DISCUSSIONS

operational TSR is reduced to 9. This reduction in TSR across the upper partial load range leads to a more efficient power production and higher power coefficients compared to conventionally applied peak-shaving approaches, e.g. solely pitching to feather before reaching the rated wind speed. Since the inner 70 % of the blades are designed for stronger winds and a TSR of 9, the aerodynamic forces are redistributed towards the blade root in the strong-wind mode which allows for more efficient peak-shaving. The early pitching and operation in strong-wind mode also lowers the thrust coefficient of the rotor. A more detailed explanation of this concept is found in Ribnitzky et al. (2024). The different design strategies for the inner and outer part of the rotor blades, also lead to an uneven distribution of the thrust along the rotor blades and corresponding imprint in the wake deficit. This feature cannot be modelled within WRF, as turbines are modelled as a disk with constant thrust across the entire rotor area.

Three variants of the IEA-15 MW turbine design are considered to assess the impact of hub height and rotor diameter of a conventional turbine design, while keeping the same rated power. Hence, we first performed simulations using the original design of the IEA-15 MW turbine, secondly with a hub height of $z_{\mathrm{hub}} = 193\,\mathrm{m}$ and with another version featuring a scaled-up design using a rotor diameter of $D = 326\,\mathrm{m}$ and a hub height of $z_{\mathrm{hub}} = 193\,\mathrm{m}$. Here, the blade design is simply upscaled without the aforementioned innovations of the HL rotor. However, the stationary aerodynamic out-of-plane bending moment is constrained to the magnitude of the IEA-15 MW design by applying conventional peak-shaving.

Figure 2 depicts the corresponding power (Fig. 2a) and thrust coefficient curves (Fig. 2b) for all investigated designs. Here, we observe a significant difference between the power curves with specific ratings of $P_{\mathrm{spec}} = 332\,\mathrm{Wm}^{-2}$ and $P_{\mathrm{spec}} = 180\,\mathrm{Wm}^{-2}$ respectively. The turbines with larger rotor diameters provide higher power production below the rated wind speed but have to be derated at wind speeds above $15\,\mathrm{ms}^{-1}$ to keep the loads within a secure operating range. The HL and upscaled IEA design show very similar performance above rated wind speed. However, below rated the HL concept has an improved power production for very low wind speeds below $5\,\mathrm{ms}^{-1}$ and wind speeds above $7.5\,\mathrm{ms}^{-1}$.

Figure 2b shows the distinct thrust characteristics of the turbine concepts. The IEA turbine employs a traditional design with a high thrust coefficient and a corresponding high wake deficit across the entire partial load range. In contrast, the HL turbine and the upscaled IEA turbine change the operating mode above $6.8\,\mathrm{ms}^{-1}$ to comply with the load constraint given by IEA-15 MW reference turbine. Therefore, the thrust coefficient drops significantly to approximately half of the value of the reference turbine. As mentioned above, the applied wind farm parametrisation requires a uniform thrust coefficient on the entire rotor of the HL turbine.

https://doi.org/10.5194/wes-2026-23
Preprint. Discussion started: 20 February 2026

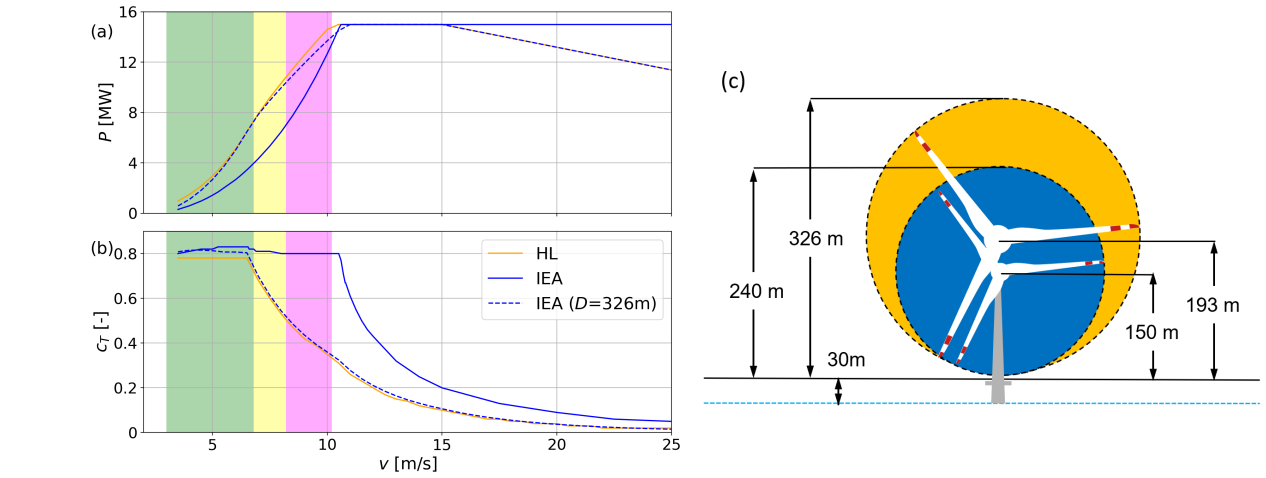

Figure 2. Power (a) and thrust coefficient (b) curves of the different design concepts used in the simulations, respectively. The HL (orange) and standard IEA (blue) turbine designs are marked by solid lines, while the upscaled IEA-15 MW turbine is depicted as a dashed blue line. The light-wind mode is shaded in green, the transition region in yellow and the strong wind mode in magenta for the HL turbine. Subfigure (c) compares the dimensions of the HL turbine (orange swept area) with the IEA turbine (blue swept area).

2.3 Wind farm layout generation

Within our study we investigate the impact of different rotor concepts for wind farm expansion plans issued by governmental offices. Thus, we select areas based on the marine spatial plans or site development plans of Germany and the Netherlands for their respective EEZs in the North Sea (Vollmer and Dörenkämper, 2024; RVO, 2025).

Within the Dutch EEZ two prominent expansion areas are present, one bordering the German EEZ in the north-east and another one bordering the Belgian EEZ in the south-west. These two areas are separated by quite some distance, leading to very small interactions between the two. Thus, we chose to not enlarge our domain any further and only include the northeastern part of the Dutch EEZ.

Regarding the placement of the turbines within the wind farm clusters considered in the German North Sea we follow two different set-ups. First, we install the same amount of turbines for both IEA-15 MW and HL turbines, i.e. keeping the same installed power density while in the second approach we reduce the amount of HL turbines in our simulations.

For the first set-up, we base our wind farm planning on the analysis of Vollmer and Dörenkämper (2024), regarding the number of turbines per cluster. Each cluster is assigned with a fixed power density, i.e., the gross amount of power installed per wind farm cluster area. After defining the installed power per area, the corresponding amount of turbines is placed in a way, that the maximum possible geometric distance between the turbines is achieved. The optimization function for the layout generation is defined by (Dörenkämper et al., 2023) as

$$f = d_{\text{mean}}^2 - (d_{\text{mean}} - d_{\text{min}})^2 - (d_{\text{mean}} - d_{\text{max}})^2 \tag{4}$$

https://doi.org/10.5194/wes-2026-23
Preprint. Discussion started: 20 February 2026

with the average distance d_{mean}, as well as minimum (d_{min}) and maximum (d_{max}) distance of each wind turbine to the closest neighbour within the wind farm cluster. The optimization aims at maximising the value of f. The layout optimization carried out is thus purely geometrical and not based on the main wind direction or potential wakes induced by nearby wind turbines or wind farms.

Figure 3 shows all the clusters within the German and Dutch EEZ. The colour coding indicates the planned power density within each wind farm cluster for the German (Fig. 3a) and Dutch EEZ (Fig. 3b), respectively. From Fig. 3a, we observe that in south-westerly direction and further away from the German coast higher capacity densities are planned compared to the clusters at the north-easterly boundaries of the EEZ.

The presented scenarios are subsequently simulated twice. Once only considering the German wind farms and secondly also including the Dutch wind farms, as they are placed upstream in the prevailing south-westerly wind direction of many German wind farms and thus heavily affecting the wind resource.

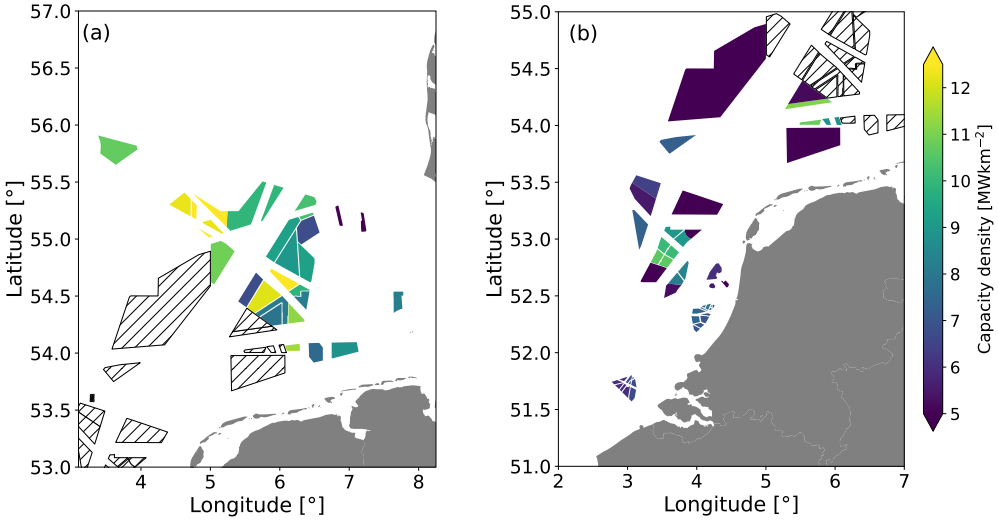

Figure 3. Planned power density of wind farms in the German (a) and Dutch (b) EEZ. The colour coding depicts the power density, while the hatched wind farms are those planned in the other country, respectively.

When basing the turbine placement purely on the planned installed capacity densities, very close turbine spacing of up to 3.1 D for the HL turbines occurs. For conventional turbines, such a small spacing could lead to an increased effective turbulence in the inflow of downstream turbines increasing the experienced fatigue loads (Sickler et al., 2023).

Thus, we follow a second approach, where we aim at reducing the installed power density within the HL-cluster, while at the same time maintaining a similar AEP to the IEA-clusters. This is achieved by reducing the number of turbines by appr. 22 % in each wind farm cluster, thus also increasing the spacing of turbines. While in the first scenario based on the installed power density, we reach an installed capacity of 70.2 GW for both types, the numbers differ for the second case. Here, we aim for an

https://doi.org/10.5194/wes-2026-23
Preprint. Discussion started: 20 February 2026

eawe european academy of wind energy
Open Access WIND ENERGY SCIENCE DISCUSSIONS

installed capacity of 54.78 GW, also resulting in a lower power density within the wind farm clusters. Again, the layout for the different clusters is obtained, by geometrically maximising the distance between the turbines.

In total, we carry out eight simulations, with different turbine placements and capacity densities as well as different adjustments to the turbine concepts themselves. Important characteristics of the resulting set-ups are shown in Table 2.

Table 2. Important characteristics of all simulations carried out within our study.

Reference code	Turbines	Specifications	Installed capacity in the German EEZ [GW]
$\mathrm{GB_{ref}}$	-	reference simulation without WFP	-
GB-IEA	IEA	standard IEA-15 MW concept	70.29
GB-HL	HL	hybrid-lambda ($z_{\mathrm{hub}} = 193\,\mathrm{m},\ D = 326\,\mathrm{m}$)	70.29
GB-IEA-HH	IEA	increased HH (z_{hub} = 193 m)	70.29
GB-IEA-D	IEA	upscaled design (z_{hub} = 193 m, D = 326 m)	70.29
$\mathrm{GB\text{-}HL_{red}}$	HL	reduced capacity	54.78
GB-NL-IEA	IEA	GB-IEA plus north-eastern Dutch farms	70.29
GB-NL-HL	HL	GB-HL plus north-eastern Dutch farms	70.29

2.4 Data post-processing and applied metrics

To evaluate the performance and ABL interaction of the turbine concepts at different conditions, we gather meteorological data like, horizontal wind speed v and wind direction ϕ from the $\mathrm{GB_{ref}}$ simulations. These quantities are taken at the centre position of each of the wind farm clusters and subsequently spatially averaged at each time step. Based on the averaged wind speed and direction, as well as the Obukhov length L, we choose four cases for further exploration.

First, we filter for situations with south-westerly wind directions and a very stable atmospheric stratification. For the wind directions we select a sector of $180° < \phi < 270°$. A situation is classified as very stable in our simulations if the Obukhov length L lies between 0 m and 200 m for at least 95 % of the included wind farm clusters. This specific threshold is based on Van Wijk et al. (1990).

Next, we separate the data set following wind speed regimes coinciding with the operating modes of the HL concept. Low wind speed situations are chosen for wind speeds between cut-in and $v < 6.8\,\mathrm{ms^{-1}}$. Medium wind speed situations, with the HL turbines operating in strong wind mode are selected for $8.3\,\mathrm{ms^{-1}} < v < 10.2\,\mathrm{ms^{-1}}$ and high wind speed situations above rated wind speed, i.e. $v > 10.2\,\mathrm{ms^{-1}}$. A summary of the filters for selected situations is presented in Table 3.

https://doi.org/10.5194/wes-2026-23
Preprint. Discussion started: 20 February 2026

eawe european academy of wind energy
Open Access WIND ENERGY SCIENCE DISCUSSIONS

Table 3. Meteorological situations defined for further analysis.

Abbreviation	Description	Conjunctive filters
WDIRSTAB	South-westerly winds and stable atmospheric stratification	$180° < \phi < 270°$ and $0\,\mathrm{m} < L < 200\,\mathrm{m}$
LW	Low wind speeds with HL turbines operating at light-wind mode	$3\,\mathrm{ms}^{-1} < v < 6.8\,\mathrm{ms}^{-1}$
SW	Medium wind speeds with HL turbines operating at strong-wind mode	$8.3\,\mathrm{ms}^{-1} < v < 10.2\,\mathrm{ms}^{-1}$
RW	Wind speeds at or above v_{rated} with HL turbines operating at rated power	$v > 10.2\,\mathrm{ms}^{-1}$

To achieve better comparability between the different rotor concepts, also considering the different shear across the rotor area, we compute the REWS. This is done for the wind fields from the simulation runs $\mathrm{GB}_{\mathrm{ref}}$, GB-IEA and GB-HL, based on the dimensions of the IEA and HL turbines respectively. The REWS (v_{eq}) as described by Wagner et al. (2014) is defined as

$$v_{\mathrm{eq}} = \left(\sum_i v_i^3 \frac{A_i}{A_{\mathrm{tot}}} \right)^{1/3} \tag{5}$$

with v the horizontal wind speed, A_i the share of the rotor area in the corresponding height band i and A_{tot} the rotor area of the considered turbine. As the drag imposed on the flow by the turbines is independent of the wind direction in the applied WFP, no wind direction correction is applied.

Subsequently, we normalise the acquired v_{eq} with v_{eq} obtained from the reference simulations $\mathrm{GB}_{\mathrm{ref}}$ following

$$v'_{\mathrm{eq}} = v_{\mathrm{eq,\,WT}} / v_{\mathrm{eq,\,ref}} \tag{6}$$

where $v_{\mathrm{eq,\,WT}}$ is the REWS of the respective turbine concept and $v_{\mathrm{eq,\,ref}}$ is the REWS from the reference simulation $\mathrm{GB}_{\mathrm{ref}}$. This is done for both turbine concepts separately. After ensuring, that the differences in REWS are smaller than the random variations between separate WRF runs, we compare the normalised v'_{eq} between the different concepts as in

$$\Delta v'_{\mathrm{eq}} = v'_{\mathrm{eq,\,IEA}} - v'_{\mathrm{eq,\,HL}} \tag{7}$$

with $v'_{\mathrm{eq,IEA}}$ and $v'_{\mathrm{eq,HL}}$ the relative wind speed reduction for the two turbine concepts. Negative values of $\Delta v'_{\mathrm{eq}}$ correspond to lower wind speed reductions of the HL turbines, i.e. lower wake effects while positive values indicate stronger wake effects.

To evaluate the performance of turbines, we also analyse the AEP, full load hours (FLH) and capacity factors (CF) of all the simulated wind farm clusters. These three metrics are computed as

$$\mathrm{AEP} = \sum_j P_j \cdot \Delta t_j \tag{8}$$

$$\mathrm{FLH} = \frac{\mathrm{AEP}}{P_{\mathrm{installed}}} \tag{9}$$

$$\mathrm{CF} = 100\,\% \cdot \frac{\mathrm{FLH}}{t_{\mathrm{tot}}} \tag{10}$$

https://doi.org/10.5194/wes-2026-23
Preprint. Discussion started: 20 February 2026

eawe european academy of wind energy
Open Access WIND ENERGY SCIENCE DISCUSSIONS

with the temporal resolution of the simulation Δt_j at each time step j, the installed power for each wind farm cluster $P_{\text{installed}}$ and the total time of the simulation t_{tot} = 8760 h. Here it is important to note, that our results do not include any further losses, e.g. electrical losses or losses due to the availability of the turbines (Dörenkämper et al., 2023).

Next to the performance we obtain from the simulations, we also compute the gross yield of the clusters AEP_{gross}. This metric does not take wake effects into account and bases the estimated power production purely on the installed power and wind speed distribution. The gross yield is computed as

$$AEP_{\text{gross}} = \sum_i P(v_i) \cdot f(v_i) \cdot P_{\text{installed}} \cdot t_{\text{tot}} \tag{11}$$

with the sum over all wind speed bins i, the power extracted from the power curve at the respective wind speed bin $P(v_i)$ and the probability for each wind speed bin $f(v_i)$.

3 Results

To analyse our results, we start by assessing the effect of the turbines on the atmospheric boundary layer itself, i.e. comparing the cluster wakes induced by the respective turbine concepts. Subsequently, we take a look at the clusters' performance indicators, such as AEP, CF and FLH for all different set-ups, before diving into the wind farm performance during doldrum events, i.e. situations with very low power production. Finally, we evaluate changes in the performance of the German farms with Dutch wind farms introduced to the simulation domains, to analyse potential cluster-wake induced performance deficits for German wind farms and how the two turbine concepts react to the changed inflow conditions from south-westerly direction.

3.1 Cluster wake effects and performance at different operating points

First, we look at the interaction of the wind farms with the ABL, mainly focusing on the reduction of the REWS induced by the wind farm clusters.

Figure 4 shows the annual average of the REWS for both scenarios GB-IEA and GB-HL. Throughout the entire domain, we observe slightly lower v_{eq} for GB-IEA. One driver for the increased REWS in the GB-HL case is the increased hub height and rotor diameter of the HL turbines, causing the integration of wind speeds at higher altitudes.

https://doi.org/10.5194/wes-2026-23
Preprint. Discussion started: 20 February 2026

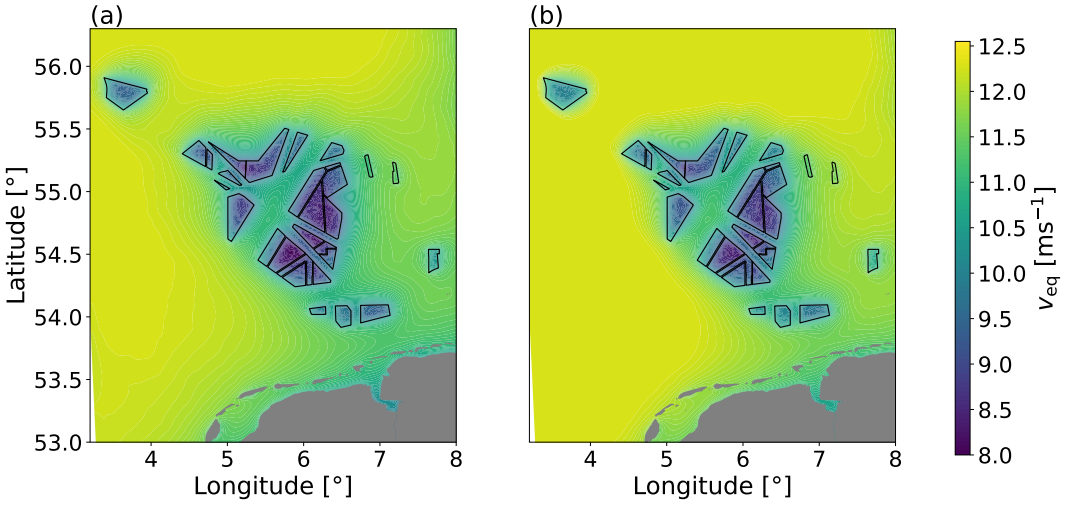

Figure 4. REWS for the simulations GB-IEA (a) and GB-HL (b) averaged across the entire year.

For a more comprehensive comparison and to correct the bias in the REWS introduced by the different hub heights and rotor diameters between the scenarios, we further analyse the difference in normalised REWS, as described in Section 2.4. Figure 5 shows the spatially resolved average difference in wind speed reduction. Here, our results show, that the HL-clusters, equipped with low-induction turbines, induce weaker wake effects within the wind farm clusters. However, outside of the cluster boundaries, the wind speed reduction is higher for the HL-clusters, due to the higher amount of extracted kinetic energy (cf. Sec. 3.2). Here, we see that although the difference is below 3 % across the German Bight clear patterns emerge from regions with high power density. Especially the far offshore N-19 cluster at the north-western boundary of the German EEZ — in the central North Sea — shows strong differences in wind speed reduction, with lower wind speed reductions for the HL-clusters. Here, the region of lower wind speed reduction, extends far into the north-easterly direction, i.e. downstream of the main wind direction within the German Bight. These pronounced differences in wake effects are also observed for the wind farm cluster located solitary at the central eastern boundary of the EEZ.

Further, a higher wind speed reduction by the HL-clusters is observed just north and to the south-west of the the N-7 and N-9 cluster in the centre of the EEZ. In south-westerly direction of these clusters wind speed reduction induced by the HL-clusters increase by up to 2 % are observed.

https://doi.org/10.5194/wes-2026-23
Preprint. Discussion started: 20 February 2026

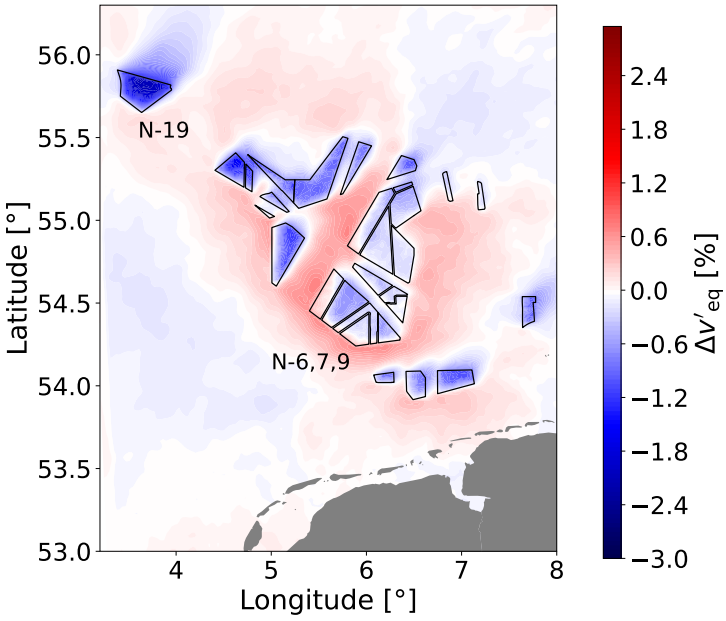

Figure 5. Difference in averaged reduction of the REWS between IEA and HL-clusters across one entire year.

In the next step, we compare the difference in cluster-induced changes of the long-term wind conditions for specific meteorological situations, i.e. different wind speed, direction and atmospheric stability regimes.

When focusing on the wind speed reductions during south-westerly wind directions and very stable stratification (WDIRSTAB) — where cluster wake effects are assumed to be strongest — we observe that the wind speed reduction induced by the HL-clusters is lower throughout almost the entire German EEZ (Fig. 6a). However, up- and downstream of the densely packed centre of the EEZ, the IEA-clusters induce weaker far-distant cluster wakes and slightly lower upstream global blockage (cf. red-shaded areas in Fig. 6a) compared to the HL-clusters. One explanation for this counter-intuitive behaviour is seen in the increased extraction of kinetic energy and higher power production from the HL-clusters due to the larger rotor diameter during these atmospheric conditions (cf. Fig. 9).

Comparing situations with different wind speed regimes, we observe that for low (Fig. 6b) and medium wind speeds (Fig. 6c), the increased production (cf. Sec. 3.2) of the HL-clusters causes a higher wind speed deficit within and in the vicinity of the clusters, with the only exception being the N-19 cluster at the far offshore north-western boundary of the EEZ. At wind speeds above rated on the other hand (Fig. 6d) the much lower thrust coefficients of the HL-clusters lead to a beneficial wind speed deficit throughout the entire German EEZ.

https://doi.org/10.5194/wes-2026-23
Preprint. Discussion started: 20 February 2026

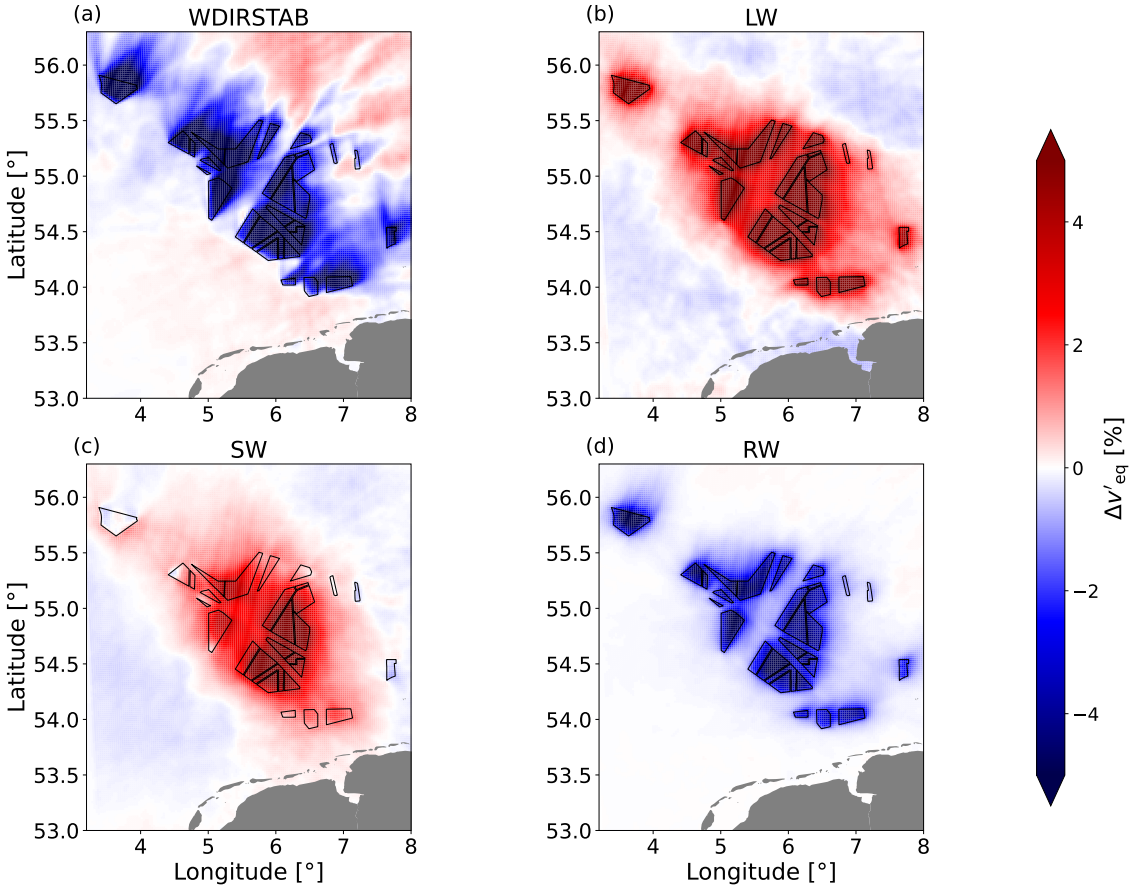

Figure 6. Difference in averaged reduction of the REWS between IEA and HL-clusters during stable stratification and south-westerly winds (a), low wind speed events (b), medium wind speeds (c) and situations with above rated wind speeds (d).

3.2 Power production and annually averaged performance

Concerning power production, we observe several differences between the two turbine concepts. Across an entire year, the AEP excluding losses due to availability, the grid and any further losses in GB-HL is 19.4 % higher compared to GB-IEA. Even when using the altered IEA concepts with increased hub height (GB-IEA-HH) and rotor diameter (GB-IEA-D) the gap is not closed entirely. While GB-IEA-HH results in an improvement of 4.3 % in AEP, in GB-IEA-D the AEP is 15.1 % higher than for the simulation with standard IEA turbines. Table 4 shows the key performance indicators for the HL turbine simulations as well as the three IEA turbine concepts.

For case GB-HL_{red} with a reduced installed capacity in the German EEZ, we observe a strongly increased average CF across all wind farm clusters. To achieve an AEP in GB-HL_{red} of 253 TWh, resembling the AEP of GB-IEA with an installed capacity of 70.2 GW across the German EEZ, a reduction of installed capacity of 22 % is possible. Despite the reduced installation capacity, the combined AEP of all clusters is only reduced by 16.5 % compared to GB-HL due to increased wind farm efficiency.

https://doi.org/10.5194/wes-2026-23
Preprint. Discussion started: 20 February 2026

eawe european academy of wind energy
Open Access WIND ENERGY SCIENCE DISCUSSIONS

Table 4. Key performance indicators for the offshore wind farms of HL (GB-HL) and IEA (GB-IEA) clusters as well as the altered IEA concepts (GB-IEA-HH, GB-IEA-D) and the scenario GB-HL_{red} with reduced number of HL turbines.

	GB-HL	GB-IEA	GB-IEA-HH	GB-IEA-D	GB-HL_{red}
AEP	303 TWh	253 TWh	264 TWh	291 TWh	253 TWh
CF	49.3 %	41.1 %	42.9 %	47.3 %	52.7 %
FLH	4313 h	3602 h	3756 h	4144 h	4544 h

Taking a look at the difference in AEP between GB-IEA and GB-HL (Fig. 7), we observe, that for each wind farm cluster, the CF is higher for GB-HL compared to GB-IEA. While HL-clusters exhibit higher AEPs at all locations, we observe larger benefits for GB-HL at locations which are located in the centre of the EEZ, i.e. at clusters affected very much by the wakes of neighbouring wind farm clusters, e.g. N-12. For rather isolated clusters, the differences are not as pronounced, as e.g. N-4, N-5 and N-19 show lower increases in AEP for GB-HL. However, no specific relation between the installed power density and CF is observed for either of the setups.

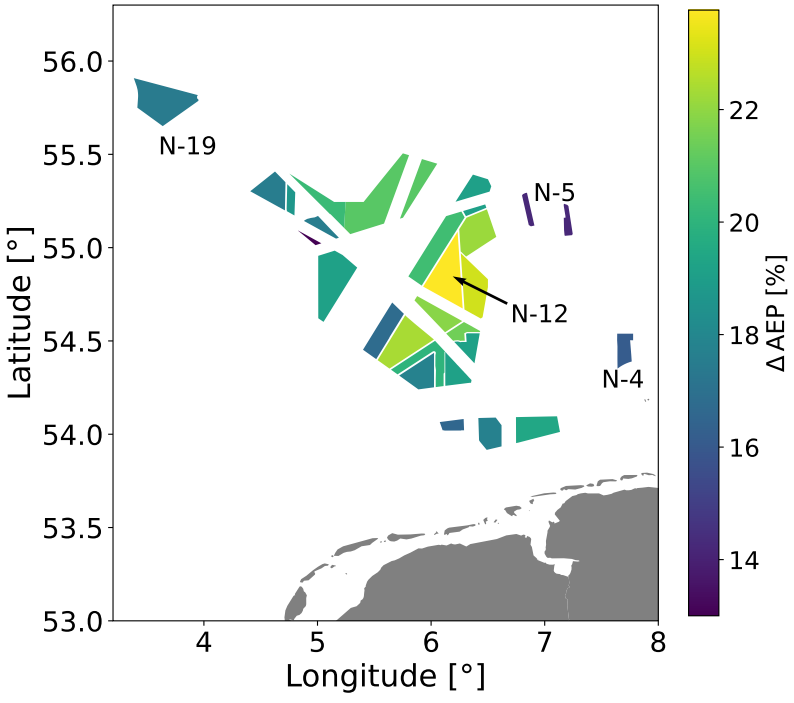

Figure 7. Difference in AEP for the all clusters respectively based on geographical location.

For a more in-depth analysis of the mesoscale effects of the turbine concepts impacting the cluster efficiency we take a closer look at four different clusters. The N-4 and N-5 clusters are rather small clusters in regions which are less affected by cluster

https://doi.org/10.5194/wes-2026-23
Preprint. Discussion started: 20 February 2026

eawe european academy of wind energy
Open Access WIND ENERGY SCIENCE DISCUSSIONS

Table 5. Fitted Weibull parameters A and k at heights of 150 m and 193 m as well as the installed power and the power density for each of the analysed wind farm clusters.

Cluster	$A_{150\,\mathrm{m}}$ [ms^{-1}]	$k_{150\,\mathrm{m}}$ [-]	$A_{193\,\mathrm{m}}$ [ms^{-1}]	$k_{193\,\mathrm{m}}$ [-]	$P_{\mathrm{installed}}$ [GW]	Power density [MW km^{-2}]
N-4	10.93	2.13	11.09	2.1	1.2	8.2
N-5	11.16	2.16	11.32	2.13	0.6	4.6
N-12	11.26	2.14	11.42	2.11	4.4	9.0
N-19	11.48	2.09	11.69	2.05	6.0	10.7

wakes and where the deployment of HL turbines shows less benefits (cf. Fig. 7). As a cluster which is considerably larger and located in a strongly cluster-wake-affected region we choose the N-12 cluster and for an isolated cluster with almost no impact of incoming cluster wakes we choose the N-19 cluster, which also has a comparatively large installed capacity.

To evaluate the gross yield, i.e. the power production of the turbines without any wake effects considered, we extract wind speed distributions at each of the four locations at the hub heights of the two turbine concepts from $\mathrm{GB}_{\mathrm{ref}}$. The fitted Weibull parameters are listed in Table 5.

Figure 8 shows the ratio of the AEP between GB-HL and GB-IEA obtained from simulations including wakes and the gross yield excluding wakes (cf. Eq. 11). Comparing the obtained results, we observe strong differences between the clusters. While the ratio between HL- and IEA-clusters also varies between the analysed clusters based on the gross yield, the results are all quite similar in the range of 1.10 to 1.16.

In the AEP ratio including wakes significantly larger differences are observed based on the characteristics and location of the cluster, with the lowest surplus at the N-5 cluster at 1.14 and the largest benefit at the strongly cluster-wake-affected N-12 cluster with a ratio of 1.25.

Smaller increases of the ratio of the AEP are observed at the N-4 and N-5 cluster. Here, the clusters themselves are comparably small and they are located quite far away from other clusters leading to lower inter- and inner-farm wake losses. The cluster N-19 also shows a high difference between gross yield and WFP ratio. This is due to the large size of the cluster itself leading to greater inner farm wake losses. The results again point out larger benefits for the HL concept in large wind farm clusters and in strongly cluster-wake-affected regions.

https://doi.org/10.5194/wes-2026-23
Preprint. Discussion started: 20 February 2026

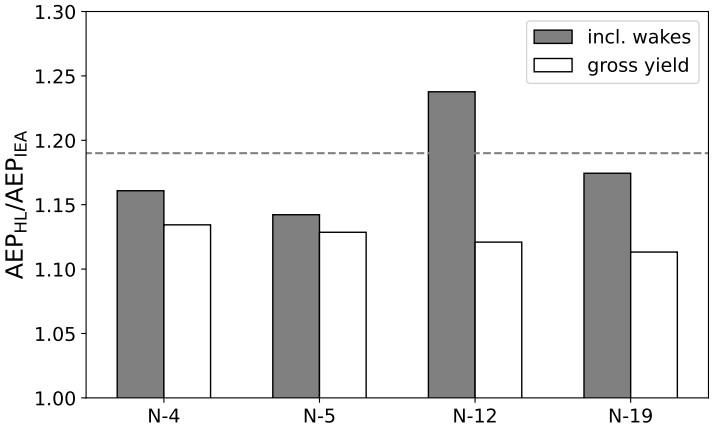

Figure 8. Ratio of the AEP as obtained from the simulation including wakes (gray) and the gross yield computation from wind speed distributions based on the reference simulation (white). The dashed black line indicates the average ratio between GB-HL and GB-IEA across all clusters from the simulation including wakes.

Next, evaluating specific meteorological situations throughout the entire year we observe differences in the performance increase of the HL-clusters. Figure 9 displays the distribution of the spatially averaged relative increase of power production from GB-HL compared to GB-IEA at each point in time for the different meteorological conditions from Table 3. Here, distinct differences in the relative power production of HL-clusters (GB-HL) compared to IEA-clusters (GB-IEA) are observed. Regarding the difference in power production during south-westerly winds and a stable ABL, we see a median increase of 42.2 % for the HL-clusters. The highest increase in performance is however observed during operation in light wind mode below 6.8 ms^{-1}. Here, the simulations show a median increase in power production of 79.5 %. However, here also the greatest spread in production difference is observed. For medium wind speeds, between the 8.2 ms^{-1} and up to rated wind speed, a median increase of 44.6 % is observed while that value decreases to 16.8 % at average wind speeds above the rated wind speed. These results show, that while power performance is increased across all wind speed regimes, the highest benefits are observed at low wind speeds, which corresponds to the design objective of the HL concept.

https://doi.org/10.5194/wes-2026-23
Preprint. Discussion started: 20 February 2026

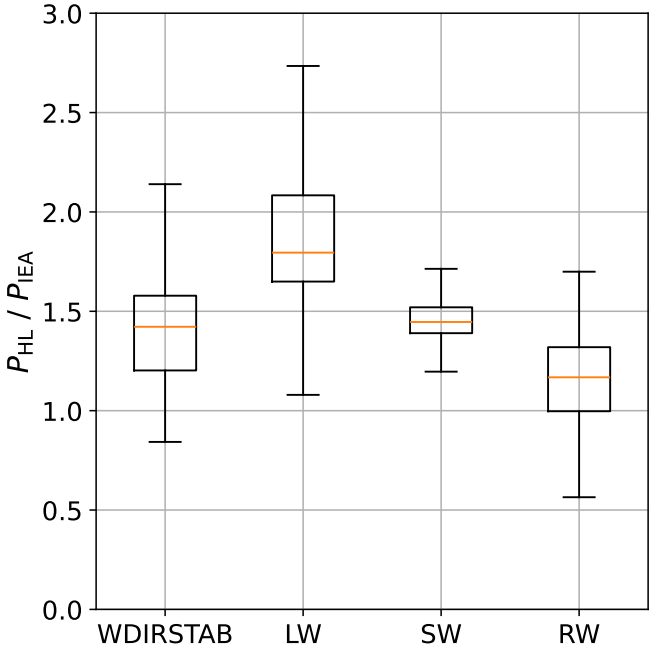

Figure 9. Boxplots of the relative power production of the HL-clusters with respect to the standard IEA. Each box represents the underlying meteorological situations from Table 3. The box limits represent the first and third quantile, respectively. The median of the respective distributions is represented by an orange line.

To analyse the temporal distribution of power production across one entire year, we use the annual duration curve (ADC). The ADC gives an indication on how many hours per year a specific power generation occurs. To generate the ADC, the power time series from the different simulation runs are each sorted in descending order and subsequently plotted over the increasing hours with the year. Figure 10 shows the ADC of the different turbine concepts. Especially in the region between 1500 h and 7000 h large increases in power production are observed for GB-HL compared to GB-IEA. In this region, the GB-HL scenario shows an 1.2 to 1.6 times higher power production compared to the GB-IEA scenario. Above approx. 2000 h per year, also the GB-HL_{red} surpasses the power production of GB-IEA. The IEA-clusters only show a surplus of power production during approx 1000 h per year, i.e. at peak production, where differences between the two concepts lie at approx only 2 %. Further, we observe that when very little wind at or below the cut-in wind speed is present, GB-HL and GB-IEA show very similar absolute power production at a lower accumulated power. When comparing the time at which both concepts are producing at least 5 % of the installed capacity, very little differences are observed. GB-HL reaches that threshold 13.7 % (1200 h) of the year, while GB-IEA reaches it 12.5 % (1095 h).

Considering the altered IEA turbines, we observe that GB-IEA-D follows the same trend as GB-HL, while power production for GB-HL is slightly higher across all the different hours. For GB-IEA-HH slight increases compared to GB-IEA are observed between 1500 h and 7000 h, but again the same trend is kept and differences to GB-HL stay large.

https://doi.org/10.5194/wes-2026-23
Preprint. Discussion started: 20 February 2026

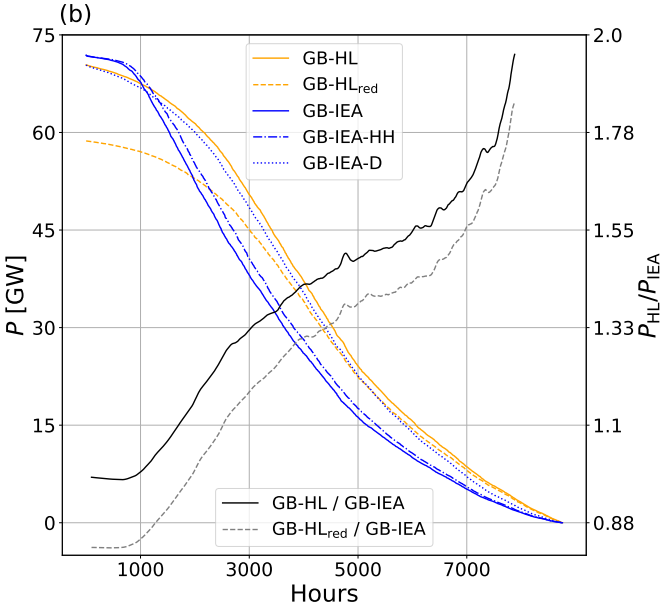

Figure 10. Annual duration curve of the different turbine concepts. Here, the cumulative number of hours in which at least a certain power production is reached is displayed. The HL-clusters (GB-HL, GB-HL$_{\mathrm{red}}$) are depicted in orange and the different IEA-based turbine variations (GB-IEA, GB-IEA-HH, GB-IEA-D) in blue. The right axis presents the ratio of power production between GB-HL and GB-IEA (black) and GB-HL$_{\mathrm{red}}$ and GB-IEA respectively (grey, dashed).

3.3 Performance during doldrum events

Next, we investigate the performance of the different turbine designs during especially challenging situations for the power system: doldrum events, i.e. time periods with very low feed-in of wind power. Note that it might be more intuitive to define
415 doldrums by a wind-speed threshold. We do not follow this, since no measurement location unaffected by the wind farm clusters (cf. met mast in power performance testing of wind turbines) can be identified that is representative of the entire German Bight. Hence, following Li et al. (2021), we apply three different levels in the definition for doldrums based on the produced power relative to the installed power. We classify them as situations where the combined power of all clusters lies below 5 %, 10 % and 20 % of the installed power respectively. Figure 11 shows the characteristics of one exemplary doldrum event.

https://doi.org/10.5194/wes-2026-23
Preprint. Discussion started: 20 February 2026

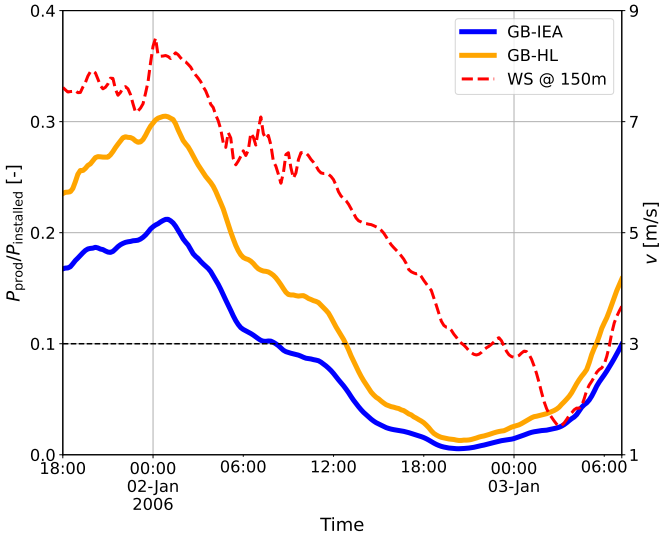

Figure 11. Exemplary doldrum event on January 2nd, 2006. Here, the power production of HL-clusters (orange) and the IEA-clusters (blue) as fraction of the installed power (left x-axis) as well as the wind speed at 150 m from GB_{ref} spatially averaged across the entire German Bight (dashed red line, right x-axis) are depicted. Further, the threshold for the 10 % doldrum is depicted as a dashed black line.

When evaluating the total number of doldrum events, i.e. situations in which the total power discretised as 10-minute averages is below the threshold, we observe clear differences between the different turbine concepts (Fig. 12a). For the most restrictive doldrum definition analysed, i.e. the 5 % definition, HL-clusters (GB-HL) exhibit approx. 15 % less doldrum events across one year compared to the different IEA-15 MW designs, which are all on a similar level. For the 10 % doldrums, the number of identified doldrum events decreases from the standard IEA (GB-IEA) design to the design with increased hub height (GB-IEA-HH) and further with increased rotor diameter (GB-IEA-D), with GB-HL again showing the least number of doldrum events. For the 20 % doldrums GB-IEA displays the highest number of identified doldrums, while GB-IEA-HH, GB-IEA-D and GB-HL all display a very similar amount of identified doldrums.

Our results further reveal, that throughout the entire year, the average duration of doldrum events is higher for GB-IEA independent of the applied definition. Fig. 12b presents, that the event duration is reduced in GB-IEA-HH and even further in GB-IEA-D for the 5 % definition. However, GB-HL exhibits an even lower doldrum duration.

Comparing the overall energy generation during doldrums detected in the GB-IEA scenario (cf. Fig. 12c), we observe strong increases for the HL-clusters. However, compared to the maximum potential energy generation, i.e. the energy that could have been generated during the doldrum events if all turbines operated at rated power (99 TWh for 5 % doldrums, 157 TWh for 10 % doldrums and 253 TWh for 20 %), all turbine concepts show very low power production.

https://doi.org/10.5194/wes-2026-23
Preprint. Discussion started: 20 February 2026

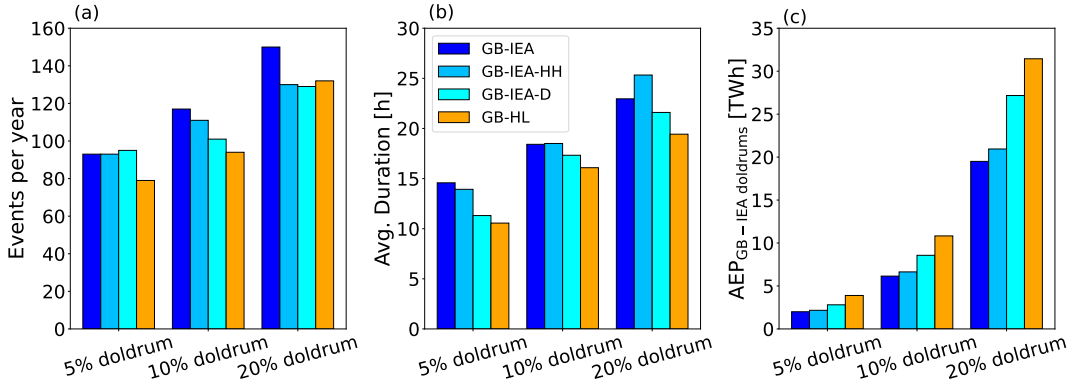

Figure 12. Number of doldrum events (a) and average doldrum duration (b). Panel (c) shows the energy generated by the four different turbine concepts during doldrums detected in the GB-IEA scenario. The IEA variants (GB-IEA, GB-IEA-HH, GB-IEA-D) are displayed in different shades of blue and GB-HL in orange.

Next, we aim at comparing the performance of the different design concepts during the same time frames. Here, we concentrate on doldrum events solely based on the GB-IEA turbines' power production, similar to Fig. 12c. Figure 13 shows the distribution of the increase of average power production of the HL-clusters during the identified doldrum events. We observe, that raising the hub height (GB-IEA-HH) and increasing the rotor diameter (GB-IEA-D) is beneficial for the energy generation during doldrum events. However, the achieved gains are only very small compared to the gains that are realised by using the HL turbines.

During the 5 % doldrums the largest increase of power production is observed, as on average the HL turbines produce 90 % more power compared to the standard IEA turbine. For higher doldrum thresholds, the benefit decreases slightly, but still, differences between the different turbine concepts are observed.

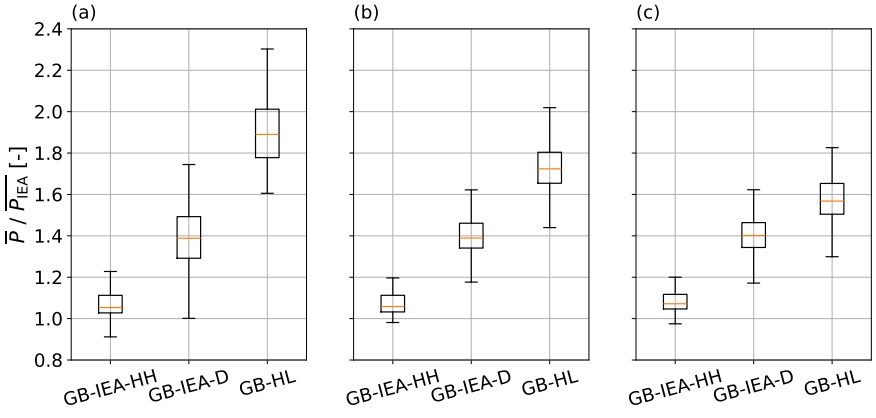

Figure 13. Box plots of the average power $\overline{P}$ of GB-IEA-HH, GB-IEA-D and GB-HL with respect to the average power of GB-IEA for the respective doldrum definitions for GB-IEA of (a) 5 %, (b) 10 % and (c) 20 % of the installed power.

https://doi.org/10.5194/wes-2026-23
Preprint. Discussion started: 20 February 2026

eawe european academy of wind energy
Open Access WIND ENERGY SCIENCE DISCUSSIONS

3.4 Influence of neighbouring wind farms in the Dutch EEZ

Lastly, to put the application of the new turbine concepts into a larger context we also implement wind farm clusters in the north-eastern part of the Dutch EEZ into our simulation. This way, we can simulate the wake effects of these farms reaching German waters and thus affecting also the German wind farm clusters. Here, each of the two turbine concepts is used across the German and Dutch EEZ respectively. Our results show, that when including Dutch wind farms, the total AEP of German wind farm clusters is reduced by 2.13 % (GB-NL-IEA) and 1.73 % (GB-NL-HL) respectively. Table 6 shows characteristic data for evaluating the performance of the wind farms both including and excluding Dutch wind farms.

Table 6. Characteristic performance indicators for the offshore wind farms of IEA and HL-clusters with and without Dutch wind farms taken into account. The relative difference is identical for AEP, CF and FLH.

	IEA			HL		
	GB-IEA	GB-NL-IEA	Difference	GB-HL	GB-NL-HL	Difference
AEP	253 TWh	248 TWh		303 TWh	298 TWh	
CF	41.1 %	40.3 %	-2.13 %	49.2 %	48.4 %	-1.73 %
FLH	3602 h	3526 h		4313 h	4239 h	

When looking at the single clusters, we observe that especially wind farm clusters at the southeastern border of the German EEZ, i.e. neighbouring the Dutch waters, exhibit a decreased performance. On the other hand, the N-4 and N-5 clusters located far away from the other clusters even show a slight increase in the CF. As expected, the losses in generated energy are lower when applying the HL turbines.

Fig. 14a shows each wind farm cluster's relative change in AEP for the IEA turbine, while Fig. 14b shows the change for the HL turbine.

https://doi.org/10.5194/wes-2026-23
Preprint. Discussion started: 20 February 2026

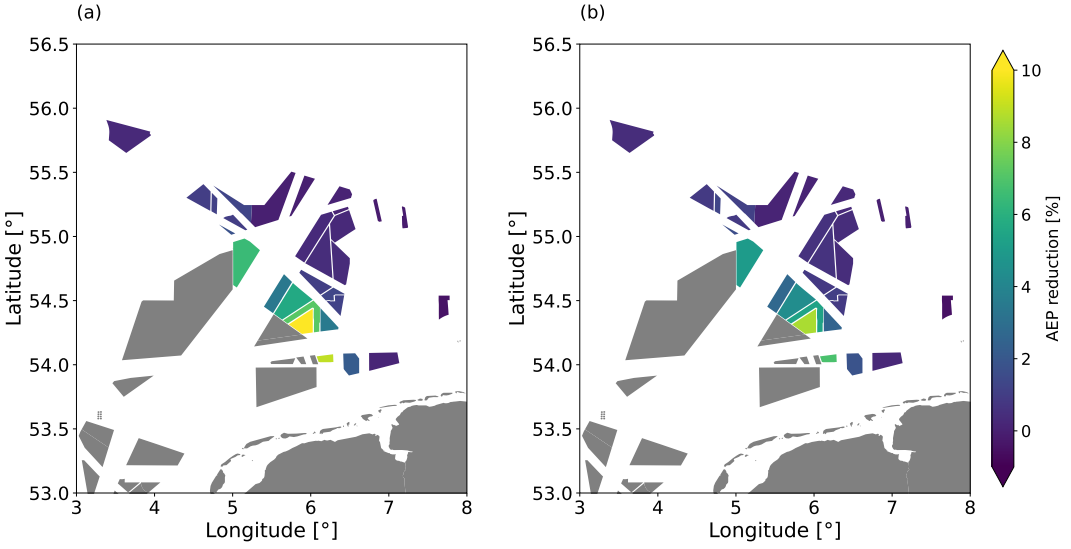

Figure 14. Change in AEP for all wind farm clusters once the Dutch wind farms are included in the simulation. The figures show the direct comparison for all clusters between GB-NL-IEA and GB-IEA (a) and GB-NL-HL and GB-HL (b) respectively.

4 Discussion

Seeking effective strategies to mitigate offshore wind farm cluster wake effects, we employed mesoscale simulations of the wind power expansion in the entire German Bight using different turbine design concepts with the same rated power of 15 MW.

Our simulations demonstrate for our target area significantly higher AEP from the same number of turbines and rated power if the low-specific-rating and low-induction HL turbine instead of the IEA-15 MW reference turbine is used. The 35 % increased rotor swept area is found to be the main reason. Moreover, the comparison to an upscaled design of a 15 MW reference turbine revealed beneficial effects in addition to the increased swept area due to the lower induction and thrust coefficient as well as the specific design and control strategy features.

Considering the average wind farm cluster wake effects in the German Bight, the innovative HL turbines show lower wind speed reductions inside the wind farms compared to the reference turbine. We attribute this observation mainly to the lower thrust coefficient of the turbines and hence weaker inner windfarm wakes. Outside of the farms the average wind speed reduction is larger for the HL turbines. Here, less energy is available in the wind, as the turbines extract more of the kinetic energy in a wider altitude range of the ABL, due to their larger rotor diameter. However, as our results reveal, the difference in wind speed reduction within as well as outside of the wind farm clusters is highly dependent on the prevailing wind speed. In case of low to medium wind speeds, until rated wind speed, the reduction is higher for HL-clusters, while it is higher for the IEA turbines during wind speeds above rated. Here, it is also important to mention, that the two rotor concepts feature significantly different hub heights and rotor diameters. While van der Laan et al. (2020) point out that normalised wake deficits are similar for rotors with different sizes within scaled flows, different shear and veer across the rotor area for both concepts lead to differences in

https://doi.org/10.5194/wes-2026-23
Preprint. Discussion started: 20 February 2026

eawe european academy of wind energy
Open Access WIND ENERGY SCIENCE DISCUSSIONS

the wake characteristics. While, we aim at reducing the influence of shear on our results by comparing the REWS, the effect of yaw misalignment of the turbines across the rotor area due to veer is not modelled within the mesoscale model.

The observed characteristics of wake development align very well with previous studies conducted for a single wind farm cluster (Paulsen et al., 2024) and also with results based on simulations of single and dual turbine setups (Ribnitzky et al., 2023), revealing several wind farm related advantages of the HL turbines compared to the IEA reference design. While the results are qualitatively comparable to higher fidelity models such as large eddy simulations (LES) and free vortex wake simulations applied by Ribnitzky et al. (2023), one drawback of using mesoscale simulations is the comparatively low resolution, resulting in a smearing out of the wake shape. Further, in contrast to the actual design of the turbine, where the axial induction and thrust coefficient vary strongly across the blade span, the thrust coefficient is modelled homogeneously across the entire rotor area in the wind turbine parametrisation in WRF. Ribnitzky et al. (2023) point out that the changes in the local thrust coefficient — which is varying along the blade span and across the operating modes — result in a strong wind speed gradient in the wake deficit at approximately 70 % of the blade span. Wind tunnel measurements of the wake development with hot-wire anemometry of Ribnitzky et al. (2023) indicate a faster wake dissipation due to an additional vortex system in the wake. Further LES are proposed to derive a more accurate wake representation in mesoscale simulations. While the resulting cluster wakes may not be affected as much by this, inner farm wake effects may be overestimated for the HL-clusters. On the other hand the mesoscale simulations, carried out in this study are able to represent the production and wake effects across one exemplary year, while higher-fidelity models, such as LES, are often restricted to shorter simulated times and smaller domains.

Further, restocking the German Bight entirely with the 15 MW turbines and keeping the targeted power densities, leads to a relatively close turbine spacing, as low as 3.1 rotor diameters for the low-specific-rating turbines. This close spacing leads to a high degree of turbulence within the inflow of downstream turbines, as well as large horizontal wind shear, as the turbines experience partial wakes. Sickler et al. (2023) show, that for inner farm distance below 4 rotor diameters, the experienced fatigue loads increase for the entire turbine, introducing the need for stronger towers and thus increasing the costs of the turbines. How the close spacing affects the loads on the HL concept can not be analysed from mesoscale simulations and needs to be assessed in future studies via higher-fidelity simulation models.

Next, we discuss the power production of the different turbine concepts. Here we observe a 19.4 % increase in gross AEP of the HL turbine compared to the standard IEA turbine. Moreover, Mehta et al. (2024) showed that optimizing a turbine design with constant rotor induction for a high AEP in offshore wind farm clusters, leads to increased rotor sizes and lower specific ratings. The application of the new HL-rotor concept, even surpasses the benefits Fliegner et al. (2025) found when redistributing the planned installation capacities across neighbouring countries to reduce wake losses by up to 18 %. While both approaches, i.e. restocking the entire German Bight with an innovative rotor concept as well as redistributing capacities across several countries, are currently not realistic in their implementation, both offer points for consideration in planning future offshore wind farm installations.

The increase in AEP for low-induction rotors (LIR) is also found by previous studies. Quinn et al. (2016) found a decreased optimum LCoE from engineering wake and integrated cost models for a large offshore cluster, as well as an AEP increase of 8 % when using the LIR. Further, Quinn et al. (2016) also found that when aiming at a similar AEP, LIR clusters need a

https://doi.org/10.5194/wes-2026-23
Preprint. Discussion started: 20 February 2026

eawe european academy of wind energy
Open Access WIND ENERGY SCIENCE DISCUSSIONS

smaller area compared to conventional turbine concepts. Compared to our study however, the authors uses the LIR design of the AVATAR project with a specific rating of $P_{\mathrm{spec}} = 300\,\mathrm{Wm}^{-2}$ and compared it to reference design from the INNWIND.EU project with $P_{\mathrm{spec}} = 400\,\mathrm{Wm}^{-2}$, while the HL-design features a significantly lower specific rating with $P_{\mathrm{spec}} = 180\,\mathrm{Wm}^{-2}$.

For a more in-depth analysis of the impact of wake effects on the difference of performance between the two rotor concepts, we also compared the spatially resolved differences in AEP between the different simulations. The beneficial effect of the HL turbines is especially pronounced in strongly cluster wake-affected areas of the German Bight with comparatively low annual average wind speeds. This effect can be further studied by comparing the gross yield, i.e. the production of an entire wind farm cluster only based on the wind speed distribution and ignoring wake effects. Here, we observe that while slight differences between the clusters at different locations are present, the benefits of the HL turbines are smaller compared to the simulations with wakes. With respect to the power density of the clusters, no significant difference in performance benefits is observed in our study, since the effects of power density and inter-cluster wakes cannot be separated from our simulation setup. Similarly, Ribnitzky et al. (2023) observed in results from LES simulations, that the benefit in the combined power production of two HL turbines is considerably higher compared to that for a single turbine.

To further investigate the mechanisms behind the increased power production, we simulated two alternative designs of the IEA turbine, once with an increased hub height and secondly with increased rotor diameter and hub height. This way, both turbine concepts, experience the same wind conditions. Note that the turbine with enlarged rotor diameter is also subject to strong peak shaving due to the same load constraints on the aerodynamic out-of-plane bending moment as the HL turbine. However, even with the upscaled IEA turbines an AEP increase of only 15.1 % is observed. This indicates, that not only the increased dimensions of the rotor, but also the new concept with two design TSRs and consequent changes in control and thrust characteristics improve the overall efficiency of wind farms, due to lower inner-farm and cluster wake effects.

Further, from the annual duration curve (ADC) and the analysis concerning the occurrence and effects of doldrums on the power production, we observe a more stable power output throughout the year, with especially beneficial performance during low winds. This specific feature could be very valuable for the future decarbonised energy system, by representing a valuable component for load balancing. The higher production at low wind speeds also provides an economic value. May et al. (2015) pointed out that with higher penetration of (offshore) wind energy in the German electricity grid the inverse correlation between wind speed and electricity price could increase, leading to higher prices during periods of low wind speeds. However, Ribnitzky et al. (2024) presented, that the new rotor design also comes with increased turbine investment costs, that are mitigated due to increased AEP and higher electricity prices during low wind speeds. Hence, analysing a single turbine without wake effects, Ribnitzky et al. (2024) observed a decrease in LCoE as well as in the cost of valued energy (COVE), i.e. a metric that also includes the value of energy for the system at given conditions, for the innovative design concept. Considering the greater costs accompanying the larger rotor and tower dimensions, but improved LCoE and COVE, the additional economic value of the new turbine concept remains to be analysed more precisely in future works.

Also, we observe that due to the increased efficiency of the HL-clusters, a reduction in installed power of up to 22 % can be achieved, while still generating the same gross AEP as for the IEA-clusters with the originally installed capacity. This lower installed capacity also bears the further advantage, that turbines are no longer erected as close together thus reducing the

https://doi.org/10.5194/wes-2026-23
Preprint. Discussion started: 20 February 2026

experienced loads. Moreover, from the ADC we see that the reduced installed capacity only leads to a lower power production throughout roughly 23 % of the time, corresponding to roughly 2000 h, across the simulated year. This aspect opens new prospects for the economic optimisation of the required off- and onshore grid expansion in Germany (Vollmer and Dörenkämper, 2025).

Concerning doldrums, the HL-clusters also prove to be beneficial, as independent of the applied power threshold to define the doldrum events, doldrums occur less often and are shorter. Further, the surplus energy generation is observed to be up to double the generation of conventional IEA turbines, depending on the applied doldrum definition. Despite the increase in observed energy generation from GB-HL to GB-IEA, our results show that also the HL-clusters only generate a small fraction of the maximum potential energy during the time of doldrums. While our study concentrates on one statistically representative year, the occurrence frequency, duration and strength of single events like doldrums is subject to fluctuations induced by climate change. While the mean wind speed across the North Sea is not expected to change significantly, a clear shift between the seasons is observed (Hahmann et al., 2022). The authors show, that throughout many different climate simulations a reduction in wind speed during the summer months is observed, while the average wind speed during the winter increases. Hence, the effect of doldrums will likely increase in the foreseeable future.

In the last part of our study, we introduced — additionally to the German wind farm areas — wind farm areas in the north-eastern part of the Dutch EEZ into our simulations. However, not all of the Dutch wind farms are considered, but only those who are located in the innermost domain of our simulation set-up — where WFP is enabled. Here, again the HL turbines have proven to be beneficial, as the reduction in AEP of the wind farms in the German EEZ due to the additional Dutch wind farms is lower compared to that in case of using the IEA turbines in all wind farms, coinciding with the improved performance at cluster-wake affected locations. However, still an additional wake loss of 1.73 % is observed within our simulations.

Future work further should aim at studying the effects leading to the increased efficiency more in-depth by employing higher fidelity large eddy simulations, also considering possible layout effects as well as the non-uniform thrust distribution across the rotor blades neglected by the mesoscale WRF model. Further, an investigation of the power production of novel rotor concepts from the perspective of system-friendliness in an energy system with different power generation and storage technologies would be of great interest.

5 Conclusion

Within our study, we show that the employment of low-specific-rating and low-induction turbines benefits not only the gross energy production but could also hold positive effects for the mitigation of cluster wakes. This benefit is driven by both the increased rotor-swept-area and the reduced inner-farm wake losses due to the lower thrust coefficient. While the gross yield of an isolated HL turbine is increased by only 12 % compared to the IEA-15 MW turbine the surplus yield is 19.4 % in the entire cluster-wake-affected German Bight. The largest increase of power production of 79.5 % is observed at low wind speeds up to 6.8 ms^{-1}. We observed, that the number and duration of identified doldrum events decreased with the HL concept compared to the IEA-15 MW turbine, while the energy generation during these events is increased by up to 90 %. The higher efficiency

https://doi.org/10.5194/wes-2026-23
Preprint. Discussion started: 20 February 2026

eawe european academy of wind energy
Open Access WIND ENERGY SCIENCE DISCUSSIONS

of the HL turbines results in a higher AEP at constant installed capacity or in the requirement of lower number of turbines and total capacity for a prescribed AEP. Moreover, our study reveals, that the HL turbines are especially beneficial in areas heavily impacted by cluster wakes in the prevailing wind directions.

The higher production at low wind speeds also shows in the distribution of power production across the year, as the HL turbine provides a more balanced power output. While the annual duration curve shows both turbine concepts converging towards larger hours, as the turbine concepts have a similar cut-in wind speed below which no power is produced, the HL concepts provides great benefits as soon as wind speeds are steadily above the cut-in wind speed.

Author contributions. JP designed the study, conducted the research and prepared the manuscript. MD contributed to the set-up of the simulations and the post-processing of the data and supervised the investigations. GS contributed significantly to the design of the study. MK contributed with supporting discussion. All co-authors thoroughly reviewed the paper.

Competing interests. The authors declare not to have any competing interests.

Acknowledgements. We acknowledge the ”Deutsche Bundesstiftung Umwelt” (DBU) as this project received funding within the scope of their PhD scholarship programme (AZ 20022/047), the SFB1463 Offshore Megastructures, funded by the Deutsche Forschungsgemeinschaft (DFG, German Research Foundation, project ID 434502799) and the C2-Wakes project by the Federal Ministry for Economic Affairs and Energy (BMWE) (grant no. 03EE3087) based on a decision of the German Bundestag. The simulations were conducted on the HPC clusters STORM and MOUSE located at the university of Oldenburg (Germany). STORM was funded through the REACT-EU programme by the NBank and the Ministry of Science and Culture (MWK) of Lower Saxony (grant no. ZW7-85186744). MOUSE is funded by the Federal Ministry for Economic Affairs and Climate Action (BMWK, Bundesministeriums für Wirtschaft und Klimaschutz) (grant no. 03EE3067A). The authors would like to acknowledge Balthazar Sengers and Lukas Vollmer for their support in setting up the mesoscale simulations, as well as Daniel Ribnitzky for the fruitful discussion in the design process of the study as well for his review of this studies results.

https://doi.org/10.5194/wes-2026-23
Preprint. Discussion started: 20 February 2026

eawe european academy of wind energy
Open Access WIND ENERGY SCIENCE DISCUSSIONS

References

Ali, K., Schultz, D. M., Revell, A., Stallard, T., and Ouro, P.: Assessment of Five Wind-Farm Parameterizations in the Weather Research and Forecasting Model: A Case Study of Wind Farms in the North Sea, Monthly Weather Review, 151, 2333–2359, https://doi.org/10.1175/MWR-D-23-0006.1, 2023.

Bortolotti, P., Johnson, N., Abbas, N. J., Anderson, E., Camarena, E., and Paquette, J.: Land-Based Wind Turbines with Flexible Rail-Transportable Blades – Part 1: Conceptual Design and Aeroservoelastic Performance, Wind Energy Science, 6, 1277–1290, https://doi.org/10.5194/wes-6-1277-2021, 2021.

Bundesnetzagentur: Marktbeobachtung - Monitoringbericht 2025, Tech. rep., Bundesnetzagentur für Elektrizität, Gas, Telekommunikation, Post und Eisenbahnen, Bonn, 2025.

Burton, T., ed.: Wind Energy: Handbook, Wiley, Chichester, repr edn., ISBN 978-0-471-48997-9, 2009.

C3S: ERA5 Hourly Data on Single Levels from 1940 to Present, https://doi.org/10.24381/CDS.ADBB2D47, 2018.

Cañadillas, B., Beckenbauer, M., Trujillo, J. J., Dörenkämper, M., Foreman, R., Neumann, T., and Lampert, A.: Offshore Wind Farm Cluster Wakes as Observed by Long-Range-Scanning Wind Lidar Measurements and Mesoscale Modeling, Wind Energy Science, 7, 1241–1262, https://doi.org/10.5194/wes-7-1241-2022, 2022.

Chaviaropoulos, P. and Sieros, G.: Design of Low Induction Rotors for Use in Large Offshore Wind Farms, in: EWEA Annual Event, Barcelona, Spain, 2014.

Dörenkämper, M., Olsen, B. T., Witha, B., Hahmann, A. N., Davis, N. N., Barcons, J., Ezber, Y., García-Bustamante, E., González-Rouco, J. F., Navarro, J., Sastre-Marugán, M., Sīle, T., Trei, W., Žagar, M., Badger, J., Gottschall, J., Sanz Rodrigo, J., and Mann, J.: The Making of the New European Wind Atlas – Part 2: Production and Evaluation, Geoscientific Model Development, 13, 5079–5102, https://doi.org/10.5194/gmd-13-5079-2020, 2020.

Dörenkämper, M., Meyer, T., Baumgärtner, D., Borowski, J., Deters, C., Dietrich, E., Fricke, J., Hans, F., Jersch, T., Leimeister, M., Neshati, M. M., Pangalos, G., Quiroz López, T. E., Quistorf, G., Requate, N., Schalk, K. V., Schmidt, J., Schnackenberg, M., Schwegmann, S., Thomas, P., Vollmer, L., Walgern, J., Widerspan, V., and Zotieieva, H.: Weiterentwicklung der Rahmenbedingungen zur Planung von Windenergieanlagen auf See und Netzanbindungssystemen, Tech. rep., Fraunhofer IWES, 2023.

Fischereit, J., Brown, R., Larsén, X. G., Badger, J., and Hawkes, G.: Review of Mesoscale Wind-Farm Parametrizations and Their Applications, Boundary-Layer Meteorology, 182, 175–224, https://doi.org/10.1007/s10546-021-00652-y, 2022.

Fitch, A. C., Olson, J. B., Lundquist, J. K., Dudhia, J., Gupta, A. K., Michalakes, J., and Barstad, I.: Local and Mesoscale Impacts of Wind Farms as Parameterized in a Mesoscale NWP Model, Monthly Weather Review, 140, 3017–3038, https://doi.org/10.1175/MWR-D-11-00352.1, 2012.

Fliegner, F. J., Kleidon, A., and Traber, T.: Cross-Border Cooperation to Mitigate Wake Losses in Offshore Wind Energy: A 2050 Case Study for the North Sea, International Journal of Energy Research, 2025, 2518 424, https://doi.org/10.1155/er/2518424, 2025.

Foloppe, B., Dewitte, L., and Munters, W.: Exploring Cooperation between Wind Farms: A Wake Steering Optimization Study of the Belgian Offshore Wind Farm Cluster, Journal of Physics: Conference Series, 2505, 012 055, https://doi.org/10.1088/1742-6596/2505/1/012055, 2023.

Gaertner, E., Rinker, J., Sethuraman, L., Zahle, F., Anderson, B., Barter, G., Abbas, N., Meng, F., Bortolotti, P., Skrzypinski, W., Scott, G., Feil, R., Bredmose, H., Dykes, K., Shields, M., Allen, C., and Viselli, A.: Definition of the IEA 15-Megawatt Offshore Reference Wind, Tech. Rep. NREL/TP-5000-75698, National Renewable Energy Laboratory (NREL), Golden, CO, 2020.

https://doi.org/10.5194/wes-2026-23
Preprint. Discussion started: 20 February 2026

Good, S., Fiedler, E., Mao, C., Martin, M. J., Maycock, A., Reid, R., Roberts-Jones, J., Searle, T., Waters, J., While, J., and Worsfold, M.: The Current Configuration of the OSTIA System for Operational Production of Foundation Sea Surface Temperature and Ice Concentration Analyses, Remote Sensing, 12, 720, https://doi.org/10.3390/rs12040720, 2020.

Gutknecht, J., Becker, M., Taschner, E., Stipa, S., Allaerts, D., Viré, A., and Van Wingerden, J.-W.: Active Cluster Wake Mixing, Journal of Physics: Conference Series, 2767, 092 052, https://doi.org/10.1088/1742-6596/2767/9/092052, 2024.

Hahmann, A. N., García-Santiago, O., and Peña, A.: Current and Future Wind Energy Resources in the North Sea According to CMIP6, Wind Energy Science, 7, 2373–2391, https://doi.org/10.5194/wes-7-2373-2022, 2022.

Hirth, L. and Müller, S.: System-Friendly Wind Power, Energy Economics, 56, 51–63, https://doi.org/10.1016/j.eneco.2016.02.016, 2016.

Iacono, M. J., Delamere, J. S., Mlawer, E. J., Shephard, M. W., Clough, S. A., and Collins, W. D.: Radiative Forcing by Long-Lived Greenhouse Gases: Calculations with the AER Radiative Transfer Models, Journal of Geophysical Research: Atmospheres, 113, https://doi.org/10.1029/2008JD009944, 2008.

Kasper, J. H. and Stevens, R. J.: Effects of Wind Turbine Rotor Tilt on Large-Scale Wind Farms, Journal of Physics: Conference Series, 2767, 092 072, https://doi.org/10.1088/1742-6596/2767/9/092072, 2024.

Li, B., Basu, S., Watson, S. J., and Russchenberg, H. W. J.: A Brief Climatology of Dunkelflaute Events over and Surrounding the North and Baltic Sea Areas, Energies, 14, 6508, https://doi.org/10.3390/en14206508, 2021.

López Prol, J., Steininger, K. W., and Zilberman, D.: The Cannibalization Effect of Wind and Solar in the California Wholesale Electricity Market, Energy Economics, 85, 104 552, https://doi.org/10.1016/j.eneco.2019.104552, 2020.

Madsen, H. A., Zahle, F., Meng, F., Barlas, T., Rasmussen, F., and Rudolf, R. T.: Initial Performance and Load Analysis of the LowWind Turbine in Comparison with a Conventional Turbine, Journal of Physics: Conference Series, 1618, 032 011, https://doi.org/10.1088/1742-6596/1618/3/032011, 2020.

May, N., Neuhoff, K., and Borggrefe, F.: Market Incentives for System-Friendly Designs of Wind Turbines, DIW Economic Bulletin, p. 10, 2015.

McCoy, A., Musial, W., Hammond, R., Hernando, D. M., Duffy, P., Beiter, P., Pérez, P., Baranowski, R., Reber, G., and Spitsen, P.: Offshore Wind Market Report: 2024 Edition, Technical Report NREL/TP-5000-90525, National Renewable Energy Laboratory (NREL), Golden, CO, 2024.

Mehta, M., Zaaijer, M., and von Terzi, D.: Drivers for Optimum Sizing of Wind Turbines for Offshore Wind Farms, Wind Energy Science, 9, 141–163, https://doi.org/10.5194/wes-9-141-2024, 2024.

Meyers, J., Bottasso, C., Dykes, K., Fleming, P., Gebraad, P., Giebel, G., Göçmen, T., and van Wingerden, J.-W.: Wind Farm Flow Control: Prospects and Challenges, Wind Energy Science, 7, 2271–2306, https://doi.org/10.5194/wes-7-2271-2022, 2022.

Nakanishi, M. and Niino, H.: Development of an Improved Turbulence Closure Model for the Atmospheric Boundary Layer, Journal of the Meteorological Society of Japan. Ser. II, 87, 895–912, https://doi.org/10.2151/jmsj.87.895, 2009.

Olson, J. B., Smirnova, T., Kenyon, J. S., Turner, D. D., Brown, J. M., Zheng, W., and Green, B. W.: A Description of the MYNN Surface-Layer Scheme, NOAA Technical Memorandum OAR GSL-67, National Oceanic and Atmospheric Administration, Boulder, CO, 2021.

Pan, Y. and Archer, C. L.: A Hybrid Wind-Farm Parametrization for Mesoscale and Climate Models, Boundary-Layer Meteorology, 168, 469–495, https://doi.org/10.1007/s10546-018-0351-9, 2018.

Paulsen, J., Dörenkämper, M., and Steinfeld, G.: Power Production and Large-Scale Wake Effects of Offshore Wind Turbines with Low Specific Rating, Journal of Physics: Conference Series, 2767, 092 060, https://doi.org/10.1088/1742-6596/2767/9/092060, 2024.

https://doi.org/10.5194/wes-2026-23
Preprint. Discussion started: 20 February 2026

Quinn, R., Schepers, G., and Bulder, B.: A Parametric Investigation Into the Effect of Low Induction Rotor (LIR) Wind Turbines on the Levelised Cost of Electricity for a 1 GW Offshore Wind Farm in a North Sea Wind Climate, Energy Procedia, 94, 164–172, https://doi.org/10.1016/j.egypro.2016.09.213, 2016.

Redfern, S., Olson, J. B., Lundquist, J. K., and Clack, C. T. M.: Incorporation of the Rotor-Equivalent Wind Speed into the Weather Research and Forecasting Model's Wind Farm Parameterization, Monthly Weather Review, 147, 1029–1046, https://doi.org/10.1175/MWR-D-18-0194.1, 2019.

Ribnitzky, D., Berger, F., and Kühn, M.: Innovative Aerodynamic Rotor Concept for Demand-Oriented Power Feed-in of Offshore Wind Turbines, Journal of Physics: Conference Series, 2265, 032 017, https://doi.org/10.1088/1742-6596/2265/3/032017, 2022.

Ribnitzky, D., Bortolotti, P., Branlard, E., and Kühn, M.: Rotor and Wake Aerodynamic Analysis of the Hybrid-Lambda Concept - an Offshore Low-Specific-Rating Rotor Concept, Journal of Physics: Conference Series, 2626, 012 008, https://doi.org/10.1088/1742-6596/2626/1/012008, 2023.

Ribnitzky, D., Berger, F., Petrović, V., and Kühn, M.: Hybrid-Lambda: A Low-Specific-Rating Rotor Concept for Offshore Wind Turbines, Wind Energy Science, 9, 359–383, https://doi.org/10.5194/wes-9-359-2024, 2024.

RVO: New Offshore Wind Farms, https://english.rvo.nl/en/topics/offshore-wind-energy/new-offshore-wind-farms, last accessed: 2025-12-16, 2025.

Sengers, B. A., Vollmer, L., and Dörenkämper, M.: Multi-Model Approach for Wind Resource Assessment, Journal of Physics: Conference Series, 2767, 092 024, https://doi.org/10.1088/1742-6596/2767/9/092024, 2024.

Sengers, B. L.: Beyond Standard Fitch: Validating WRF's Wind Farm Parameterizations with Offshore SCADA Data, 2025.

Sickler, M., Ummels, B., Zaaijer, M., Schmehl, R., and Dykes, K.: Offshore Wind Farm Optimisation: A Comparison of Performance between Regular and Irregular Wind Turbine Layouts, Wind Energy Science, 8, 1225–1233, https://doi.org/10.5194/wes-8-1225-2023, 2023.

Skamarock, C., Klemp, B., Dudhia, J., Gill, O., Liu, Z., Berner, J., Wang, W., Powers, G., Duda, G., Barker, D., and Huang, X.-y.: A Description of the Advanced Research WRF Model Version 4, Tech. Rep. NCAR/TN-556+STR, NCAR, Boulder, CO, 2021.

Syed, A. H., Javed, A., Asim Feroz, R. M., and Calhoun, R.: Partial Repowering Analysis of a Wind Farm by Turbine Hub Height Variation to Mitigate Neighboring Wind Farm Wake Interference Using Mesoscale Simulations, Applied Energy, 268, 115 050, https://doi.org/10.1016/j.apenergy.2020.115050, 2020.

Tyagi, D. and Schmitz, S.: Amendment to Glauert's Optimum Rotor Disk Solution, in: 2024 Regional Student Conferences, American Institute of Aeronautics and Astronautics, Multiple Locations, ISBN 978-1-62410-730-6, https://doi.org/10.2514/6.2024-84552, 2024.

van der Laan, M., Andersen, S., Kelly, M., and Baungaard, M.: Fluid Scaling Laws of Idealized Wind Farm Simulations, Journal of Physics: Conference Series, 1618, 062 018, https://doi.org/10.1088/1742-6596/1618/6/062018, 2020.

Van Wijk, A. J. M., Beljaars, A. C. M., Holtslag, A. A. M., and Turkenburg, W. C.: Evaluation of Stability Corrections in Wind Speed Profiles over the North Sea, Journal of Wind Engineering and Industrial Aerodynamics, 33, 551–566, https://doi.org/10.1016/0167-6105(90)90007-Y, 1990.

Volker, P. J. H., Badger, J., Hahmann, A. N., and Ott, S.: The Explicit Wake Parametrisation V1.0: A Wind Farm Parametrisation in the Mesoscale Model WRF, Geoscientific Model Development, 8, 3715–3731, https://doi.org/10.5194/gmd-8-3715-2015, 2015.

Vollmer, L. and Dörenkämper, M.: Ad-Hoc Analyse: Ertragsmodellierung der Ausbauszenarien 22 und 23, Tech. rep., Fraunhofer IWES, Bremerhaven, https://www.bsh.de/DE/THEMEN/Offshore/Meeresfachplanung/Laufende_Fortschreibung_Flaechenentwicklungsplan/Anlagen/Downloads_Entwurf_FEP/Adhoc_Analyse_Ertragsmodellg_22_23.html, 2024.

https://doi.org/10.5194/wes-2026-23
Preprint. Discussion started: 20 February 2026

Vollmer, L. and Dörenkämper, M.: Optimierung Der Verteilung von Offshore-Netzanbindungssystemen Und Windparkleistung Für Den Netzentwicklungsplan Strom 2037/2045 (Version 2025), Tech. rep., Fraunhofer IWES, Oldenburg, https://www.netzentwicklungsplan.de/StudieOptimierungIWES, last accessed: 27.01.2026, 2025.

Vollmer, L., Sengers, B. A. M., and Dörenkämper, M.: Brief Communication: A Simple Axial Induction Modification to the Weather Research and Forecasting Fitch Wind Farm Parameterization, Wind Energy Science, 9, 1689–1693, https://doi.org/10.5194/wes-9-1689-2024, 2024.

Wagner, R., Cañadillas, B., Clifton, A., Feeney, S., Nygaard, N., Poodt, M., Martin, C. S., Tüxen, E., and Wagenaar, J. W.: Rotor Equivalent Wind Speed for Power Curve Measurement – Comparative Exercise for IEA Wind Annex 32, Journal of Physics: Conference Series, 524, 012 108, https://doi.org/10.1088/1742-6596/524/1/012108, 2014.